



TRABALHO DE CONCLUSÃO DE CURSO

**ANALYSIS OF
FILTERED OFDM FOR 5G**

Lucas Baião Pires

Brasília, Junho de 2018

UNIVERSIDADE DE BRASÍLIA

FACULDADE DE TECNOLOGIA

UNIVERSIDADE DE BRASÍLIA
Faculdade de Tecnologia

TRABALHO DE CONCLUSÃO DE CURSO

**ANALYSIS OF
FILTERED OFDM FOR 5G**

Lucas Baião Pires

*Relatório submetido ao Departamento de Engenharia
Elétrica como requisito parcial para obtenção
do grau de Engenheiro Eletricista*

Banca Examinadora

Prof. André Noll Barreto, ENE/UnB

Orientador

Prof. João Paulo Leite, ENE/UnB

Examinador interno

Prof. Paulo Henrique P. de Carvalho, ENE/UnB

Examinador interno

Dedicatória

Dedico à minha mãe Laine, ao meu pai Lísias, aos meus irmãos Lúvia, Victor e Vinícius, ao meu primo Fernando e ao meu tio Tito.

Lucas Baião Pires

Agradecimentos

Agradeço aos meus pais, Laine e Lísias, por todo apoio, amor, carinho e ensinamentos que sempre me deram, ao longo de todos esses anos, mesmo nos momentos mais difíceis. Aos meus irmãos, irmã e primo, Lívia, Victor, Vinícius e Fernando, agradeço por todos os bons momentos de descontração que temos juntos.

Agradeço ao meu tio Tito por todo o carinho, suporte, conversas e ideias "viajadas" ao longo da minha vida.

Por todos os "dogões" e por compartilharem de toda essa experiência, que foram todos esses anos na engenharia, agradeço aos meus colegas de jornada, Caio, Frank, João Paulo, Alex, Arthur e Pedro.

Por fim, sou grato ao professor André Noll, por me orientar ao longo deste trabalho de conclusão de curso.

Lucas Baião Pires

RESUMO

A quarta geração de comunicações móveis, 4G, proveu conexões com altas velocidades, taxas de dados e resiliência na última década. No entanto, novas tecnologias estão surgindo e estas popularizarão-se no futuro próximo. Tecnologias como veículos autônomos, monitoramento de saúde, jogos online e Internet das Coisas (IoT) demandarão altíssimas taxas de dados (20 Gbps), baixíssima latência (1 ms) e baixo consumo de energia. Para atender a estes requisitos, é esperada uma mudança de paradigma em telecomunicações. O OFDM filtrado (fOFDM) traz uma redução considerável das radiações fora de banda, possibilitando a divisão do espectro em sub-bandas, que possuem numerologias independentes e podem ser transmitidas sem a necessidade de sincronia global. Deste modo, esta forma de onda visa atender as mais heterogêneas aplicações na interface aérea da quinta geração (5G), além de aumentar a eficiência espectral dos sistemas de telecomunicações. Neste trabalho, o desempenho do fOFDM foi avaliado, por meio de simulações computacionais, sob diversas circunstâncias, tais como propagação com multipercorso, interferência, transmissão assíncrona, diferentes filtros, etc. Os resultados destes estudos são comparados ao OFDM, para que se tenha uma melhor percepção das diferenças entre as duas tecnologias.

ABSTRACT

The fourth generation of mobile communications (4G) provided high speed, high bit rate and resilient connections for the last decade. However, new technologies are appearing and they are expected to become popular in the near future. Technologies like autonomous vehicles, health care monitoring, online gaming and Internet of Things (IoT) will demand high bit rates (20 Gbps), ultra-low latency (1 ms) and low power consumption. In order to attend these requirements, a paradigm shift is expected in telecommunications. Filtered OFDM (fOFDM) brings a considerable out-of-band emission (OOBE) reduction, making it possible to divide the spectrum into sub-bands, which have independent numerology and may be transmitted without the need of global synchrony. Therefore, this waveform seeks to support the most heterogeneous applications, while also enhancing the system's spectral efficiency. In this work, fOFDM's performance was studied, by computational simulations, under diverse circumstances, e.g., multipath propagation, interference, asynchronous transmission, different filters, etc. The investigations results are compared to OFDM, in order to attain a better perception of the differences between the two technologies.

SUMMARY

1	INTRODUCTION	1
1.1	CONTEXT	1
1.2	PROBLEM STATEMENT	3
1.3	OUTLINE	3
2	OFDM AND FOFDM	5
2.1	INTRODUCTION	5
2.2	OFDM	5
2.2.1	INTRODUCTION	5
2.2.2	FREQUENCY CHOICE AND ORTHOGONALITY	7
2.2.3	IDFT AND DFT	7
2.2.4	THE CYCLIC PREFIX	8
2.2.5	SINGLE TAP EQUALIZER	8
2.2.6	CODING AND INTERLEAVING	10
2.2.7	TRANSMISSION AND RECEPTION: D/A AND A/D CONVERSIONS AND FREQUENCY MIXING	10
2.2.8	OVERALL ANALYSIS	10
2.3	FOFDM	12
2.3.1	INTRODUCTION	12
2.3.2	FLEXIBILITY	12
2.3.3	TRANSCEIVER STRUCTURE	13
2.3.4	FILTER DESIGN AND IMPLEMENTATION	15
3	FIR FILTERS	16
3.1	CAUSAL FILTERS	16
3.2	THE WINDOW METHOD	18
4	THE HERMES SIMULATOR	22
4.1	ABOUT HERMES	22
4.2	SAMPLING	23
4.2.1	SINGLE SIGNAL TRANSMISSION	23
4.2.2	MULTIPLE SIGNALS TRANSMISSION	25
4.3	FRAME STRUCTURE	26

5	SIMULATION RESULTS	28
5.1	FILTER DESIGN IMPACT ON FOFDM PERFORMANCE	28
5.1.1	WINDOW IMPACT ON FOFDM PERFORMANCE	29
5.1.2	FILTER ORDER EFFECTS	30
5.2	MULTIPATH PROPAGATION.....	33
5.3	SYNCHRONOUS TRANSMISSION UNDER ADJACENT-CHANNEL INTERFERENCE....	37
5.4	ASYNCHRONOUS TRANSMISSION UNDER ADJACENT-CHANNEL INTERFERENCE..	38
6	CONCLUSIONS	45
6.1	FUTURE WORKS.....	45
	BIBLIOGRAPHY	47

LISTA DE FIGURAS

1.1	ITU's vision on the enhancement from IMT-Advanced to IMT-2020 [1].	2
2.1	Block diagram of an OFDM system for wireless communication. Inspired by [2].	6
2.2	Illustration of an OFDM signal's spectrum with $K = 4$ subcarriers. The subcarriers are spaced by Δf .	7
2.3	OFDM symbols in a multipath channel. Inspired by [2].	9
2.4	Illustration of a spectrum division into sub-bands.	13
2.5	FOFDM resource allocation. Extracted from [3].	14
2.6	Downlink transceiver structure of fOFDM. Extracted from [3].	14
3.1	Simple brick wall filter.	16
3.2	Truncated sinc.	17
3.3	Shorter truncated sinc generating a lesser quality filter.	17
3.4	Longer truncated sinc generating a higher quality filter.	18
3.5	Window's size effects on magnitude response.	19
3.6	FIR filter's magnitude response with different windows.	20
3.7	FIR filter's impulse response with different windows.	21
4.1	Illustration of signal $y_1(t)$.	23
4.2	Complex envelope of $y_1(t)$.	24
4.3	Passband representation of $y(t)$.	25
4.4	Baseband representation of $y(t)$.	26
4.5	Frame structure illustration.	27
5.1	BER obtained by simulating the transmission of fOFDM, with different filters, and OFDM symbols.	29
5.2	BER obtained by simulating the transmission of fOFDM, with different filters, and OFDM symbols. Each simulation run was composed of two signals with the same technology and a frequency separation of 30 kHz.	30
5.3	FOFDM and OFDM in synchronous transmission. $ISR = 10\text{dB}$.	31
5.4	FOFDM and OFDM in asynchronous transmission. $ISR = 10\text{dB}$.	31
5.5	Comparison between fOFDM and OFDM signals in the frequency domain. In this case, fOFDM's OOB was 20dB lower than OFDM's.	32
5.6	Comparison between two fOFDM signals in the frequency domain with different filter orders. Notice how the spectrum decay is faster for the higher order filter.	32

5.7	Zooming over the spectrum decays presented in Figure 5.6, so the reader may take a better look over the differences between the signals.	33
5.8	FOFDM's performance under asynchronous transmission. ISR and guard band are fixed while the filter order M is varied.	34
5.9	FOFDM's performance under asynchronous transmission. ISR and guard band are fixed while the filter order M is varied.	34
5.10	FOFDM's performance under asynchronous transmission. ISR and guard band are fixed while the filter order M is varied, with a doubled CP length.	35
5.11	FIR filter with different orders.	35
5.12	BER obtained by simulating the transmission of fOFDM, with different filters, and OFDM symbols.....	36
5.13	BER obtained by simulating the transmission of fOFDM, with different filters, and OFDM symbols.....	37
5.14	BER obtained by simulating OFDM and fOFDM symbols transmissions under interference with a single tone guard band between main signal and interfering signal. ISR = 0dB.....	39
5.15	BER obtained by simulating OFDM and fOFDM symbols transmissions under interference with a single tone guard band between main signal and interfering signal. ISR = 10dB.	39
5.16	BER obtained by simulating OFDM and fOFDM symbols asynchronous transmissions under interference with a half-symbol delay present on the interfering signal. Guard band = 1 tone.	40
5.17	BER obtained by simulating OFDM and fOFDM symbols asynchronous transmissions under interference with a half-symbol delay present on the interfering signal. Multiple guard bands were simulated.....	41
5.18	BLER obtained by simulating OFDM and fOFDM symbols asynchronous transmissions under interference with a half-symbol delay present on the interfering signal. Multiple guard bands were simulated.....	41
5.19	BER obtained by simulating OFDM and fOFDM symbols transmissions under interference with a single tone guard band between main signal and interfering signals. ISR = 0dB.....	42
5.20	BER obtained by simulating OFDM and fOFDM symbols transmissions under interference with a two-tones guard band between main signal and interfering signals. ISR = 10dB.	43
5.21	BER obtained by simulating OFDM and fOFDM symbols transmissions under interference with a two tones guard band between main signal and interfering signals. ISR = 20dB.	43

LISTA DE TABELAS

5.1	Parameters table.....	28
5.2	Parameters table.....	38

Abbreviations / Glossary

3GPP	<i>3rd Generation Partnership Project</i>
4G	<i>4th generation</i>
5G	<i>5th generation</i>
AWGN	<i>Additive white Gaussian noise</i>
BER	<i>Bit Error Rate</i>
BLER	<i>Block Error Rate</i>
CP	<i>Cyclic Prefix</i>
DSL	<i>Digital Subscriber Line</i>
DFT	<i>Discrete Fourier Transform</i>
IDFT	<i>Inverse Discrete Fourier Transform</i>
FFT	<i>Fast Fourier Transform</i>
fOFDM	<i>Filtered Orthogonal Division Multiplexing</i>
FBMC	<i>Filter Bank Multicarrier</i>
GFDM	<i>Generalized Frequency-Division Multiplexing</i>
HERMES	<i>Heterogeneous Radio Mobile Simulator</i>
ICI	<i>Intercarrier Interference</i>
IEEE	<i>Institute of Electrical and Electronics Engineers</i>
ITU	<i>International Telecommunication Union</i>
ITU-R	<i>International Telecommunication Union - Radio group</i>
IMT	<i>International Mobile Telecommunications</i>
IMT-A	<i>International Mobile Telecommunications Advanced</i>
IMT-2020	<i>International Mobile Telecommunications for 2020</i>
ISI	<i>Inter-symbolic Interference</i>
ISR	<i>Interference-to-signal Ratio</i>
MIMO	<i>Multiple-Input Multiple-Output</i>
OFDM	<i>Orthogonal Frequency-Division Multiplexing</i>
OFDMA	<i>Orthogonal Frequency-Division Multiplexing / Multiple Access</i>
OOBE	<i>Out-of-Band Emission</i>
PSK	<i>Phase Shift Keying</i>
QAM	<i>Quadrature Amplitude Modulation</i>
S/P	<i>Serial-to-parallel</i>
TA	<i>Time Advance</i>
TTI	<i>Transmit-Time Travel</i>
UFMC	<i>Universal-Filtered Multicarrier</i>
WIMAX	<i>Worldwide Interoperability for Microwave Access</i>
WLAN	<i>Wireless Local-Area Network</i>
WOOFDM	<i>Windowed OFDM</i>

Chapter 1

Introduction

1.1 Context

Since it was released, the 4G Long Term Evolution (LTE) has brought many high-quality services for the consumers. According to the International Telecommunication Union - Radio Sector (ITU-R) [4], a full International Mobile Telecommunications-Advanced (IMT-A) system should be able to provide data rates up to 100 Mbit/s for low and 1 Mbit/s for high mobility. The communications structure must allow advanced mobile services, low- to high-mobility applications and a large range of data rates, according to user demands, in diverse scenarios.

A great deal of 4G's commercial success is due to its waveform, the orthogonal frequency division multiplexing (OFDM). OFDM provides channel resiliency, efficient digital implementation, multiple access and simple equalization [2, 5]. All of these characteristics made it possible for LTE to achieve such high data rates.

Nowadays, LTE Advanced (LTE-A) is capable of delivering 3 Gbit/s in the downlink and 1.5 Gbit/s in the uplink, by making use of techniques such as carrier-aggregation and multiple-input multiple-output (MIMO). LTE is also being adapted to provide device-to-device communication, in order to support Internet of Things (IoT) applications [6].

Even though 4G has been a success, new applications and demands have appeared, raising the need for a new breakthrough in mobile telecommunication systems. The current system is coming to its performance limits, not only because of traffic and amount of users but also because of new applications that hadn't been designed by the time LTE was conceived [6]. Applications such as IoT, steering and control via wireless communication links, mobile gaming, remote control of robots, autonomous driving and health care monitoring are some of the examples of the services that current technology cannot support. These applications demand round trip times (RTT) around 1 ms [7].

By the time this work has been written, 5G has not yet been fully standardized by ITU. The first standard version is due in 2020 [1]. However, there are ongoing standardization activities [8].

In 2015, ITU released its vision about the IMT-2020 (5G) technology development [1] and how

Enhancement of key capabilities from IMT-Advanced to IMT-2020

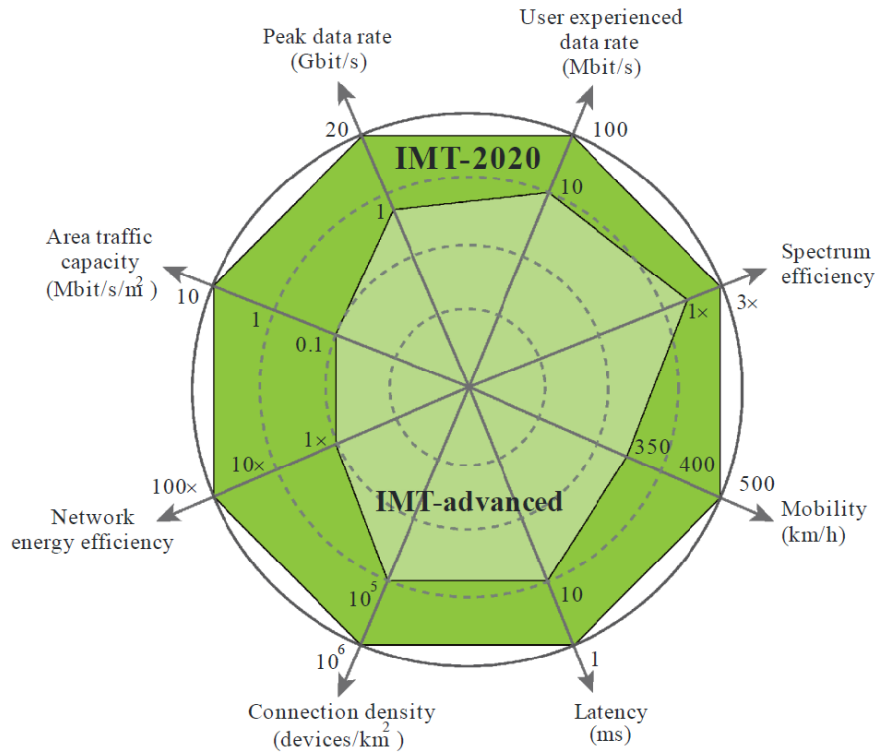


Figure 1.1: ITU's vision on the enhancement from IMT-Advanced to IMT-2020 [1].

it should surpass IMT-Advanced (4G). Figure 1.1 portrays this comparison. The values in Figure 1.1 are targets for IMT-2020 and may still be revised in future studies.

According to ITU [1], IMT-2020 is expected to provide peak data rates of 10 Gbit/s and, under certain conditions, it shall support up to 20 Gbit/s peak data rate. The data rate experienced by the user should be of 100 Mbit/s for wide coverage, e.g., urban areas. 1 Gbit/s, indoor, should be obtainable in hotspot cases. Spectrum efficiency should increase by three times when compared with 4G. An area traffic capacity of 10 Mbit/s/m², in hotspots, is expected. The energy consumption is not to increase beyond the current numbers, while providing all the enhanced performance. An 1 ms over-the-air latency should be possible in IMT-2020, supporting real-time response applications. Mobility up to 500km/h should be backed by the technology while maintaining acceptable quality of service (QoS). This is envisioned in particular for high speed trains. Lastly, 5G is expected to support a connection density up to 10⁶/km², e.g., massive machine-to-machine communications.

In order to achieve all the desired specifications, radio network architectural changes are to be proposed in comparison with 4G, such as cloud radio access networks, distributed antenna systems and virtual cells. IMT-2020 will deal with different and more complex scenarios like machine-type communications, vehicular communications and heterogeneous networks (HetNets). The latter is already covered in 4G but will have an increased importance in 5G [6].

In addition, it is likely that structural improvements will happen in the lower layers of the air interface, the physical (PHY) and MAC layers [6], e.g., utilization of new waveforms, new frame

structures, interference mitigation. In order to achieve the expected data rate and throughput, it is necessary to enhance the system's spectral efficiency and bandwidth.

1.2 Problem Statement

The 5G technology has ambitious goals and there is the need of developing and implementing techniques, in different areas, so the next generation of mobile communications may be realized.

Due to 5G's requirements, a flexible waveform, that may support heterogeneous applications, with different requirements, must be implemented. However, though OFDM may be used to provide high-data-rate and low-latency communications, it is not a flexible scheme. Conventional OFDM requires global synchronization between users and stations, as well fixed numerology in order to obtain time orthogonalization. Therefore, OFDM is not able to, simultaneously, suit the needs of diverse applications, with different specifications.

There are different waveforms that are candidates for 5G standard, e.g., windowed-OFDM (wOFDM), universal filtered multi-carrier (UFMC), filtered OFDM (fOFDM), filter bank multi-carrier modulation (FBMC) and general frequency division multiplexing (GFDM).

Among the cited waveforms, fOFDM provides a smoother transition from OFDM. FOFDM does not increase system complexity, such as in FBMC and GFDM cases. The scheme can coexist with MIMO transmission and also provides better OOB than wOFDM and UFMC. The drawback, in comparison with wOFDM and UFMC, is its increased complexity due to the filtering operation. A more in-depth comparison between waveforms is provided by [9].

A possible candidate as 5G standard communication scheme is the filtered OFDM (fOFDM). FOFDM is designed in order to raise spectral efficiency and resource flexibility, suiting the numerous heterogeneous applications that will appear for 5G to support.

Therefore, investigating fOFDM performance in diverse scenarios and comparing it to its predecessor, OFDM, is of interest, so fOFDM advantages and drawbacks may be verified.

In this work, fOFDM's performance is studied in diverse scenarios: transmission under interference, different filters, asynchronous transmissions and multipath propagation, by computational simulations ran by the Heterogeneous Radio Mobile Simulator (HERMES).

1.3 Outline

Chapter 2 discusses OFDM and fOFDM, presenting the theoretical framework behind each of the schemes, the advantages and drawbacks that the waveforms provide.

Next, Chapter 3 discusses FIR filters and its application in fOFDM, while presenting the design technique.

Chapter 4 presents the HERMES simulator, which is the computational simulator that performed all the simulations in this text. The chapter also discusses the theory behind some important

aspects that power up the simulator.

Following, Chapter 5 exhibits the most critical section in this work, which are the obtained results and conclusions made about the fOFDM waveform.

Lastly, Chapter 6 contains the conclusions about the overall results in this work.

Chapter 2

OFDM and FOFDM

2.1 Introduction

4G technology has provided resilient, mobile and fast connection to society. A key factor for its success is the OFDM waveform. This waveform has many benefits, that are vastly explored nowadays. In the near future, applications and services such as IoT, vehicle communication, mobile gaming and many others, will demand data rates and latency that 4G will not be able to satisfy.

Although OFDM has been a huge success, its high OOB and inflexibility make room for improvements. Hence, alternative waveforms are being studied to replace OFDM and become the new 5G standard, such as fOFDM.

Throughout this chapter, OFDM and fOFDM will be defined and described.

2.2 OFDM

2.2.1 Introduction

Orthogonal frequency division multiplexing (OFDM) is one of the most important communication schemes nowadays. Present in many largely used systems, it has many advantages like multipath propagation resiliency, efficient digital implementation and the possibility of high-data rate transmission. Some drawbacks in this technique are high peak-to-average power ratio (PAPR) [10], numerology rigidity and sensitivity to frequency and time synchronization problems.

In this text, numerology is the set of OFDM's numerical parameters, which are cyclic prefix size, subcarrier spacing, modulation order, coding rate, symbol time interval, FFT length and subcarriers amount.

OFDM's first two main concepts [2], which are usage of parallel data transmission and frequency multiplexing [11] and orthogonal signals generation using the fast fourier transform (FFT) [12], were published in the mid-1960s. Next, in the mid-1980s, the third main concept, the cyclic prefix, was conceived [13]. After more than thirty years of research and development, OFDM has been

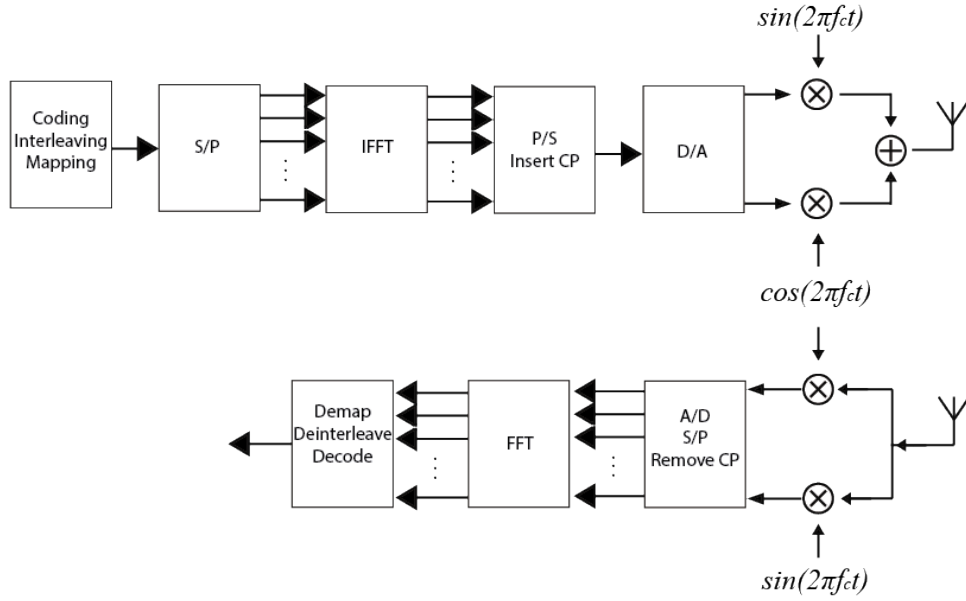


Figure 2.1: Block diagram of an OFDM system for wireless communication. Inspired by [2]

widely implemented in high-speed digital communications. For its resiliency in different channels and delivered high data rates, OFDM is used in many applications. Some of the technologies that rely on it are: wireless local area network (WLAN) technologies based on the Institute of Electrical and Electronics Engineers (IEEE) 802.11a, 802.11g, 802.11n, 802.11ac, and 802.11ad standards, 3rd Generation Partnership Project Long Term Evolution (3GPP LTE), Digital Subscriber Line (DSL) internet access, Worldwide Interoperability for Microwave Access (WiMAX), power line communications, and others [2, 5].

In this section, OFDM transmission and reception are briefly described. A general diagram illustrating the whole scheme is displayed in Figure 2.1.

A general OFDM $x(t)$ signal, with K subcarriers may be described by

$$x(t) = g_{rec}(t) \sum_{k=0}^{K-1} a_k e^{j2\pi f_k t} \quad (2.1)$$

In equation 2.2.1, $g_{rec}(t)$ is the standard rectangular pulse, f_k is the subcarrier frequency, and a_k is given by

$$a_k = a_{k,I} + ja_{k,Q}, \quad k = 0, 1, \dots, K - 1 \quad (2.2)$$

a_k contains the constellation coordinates in $(a_{k,I}, a_{k,Q})$.

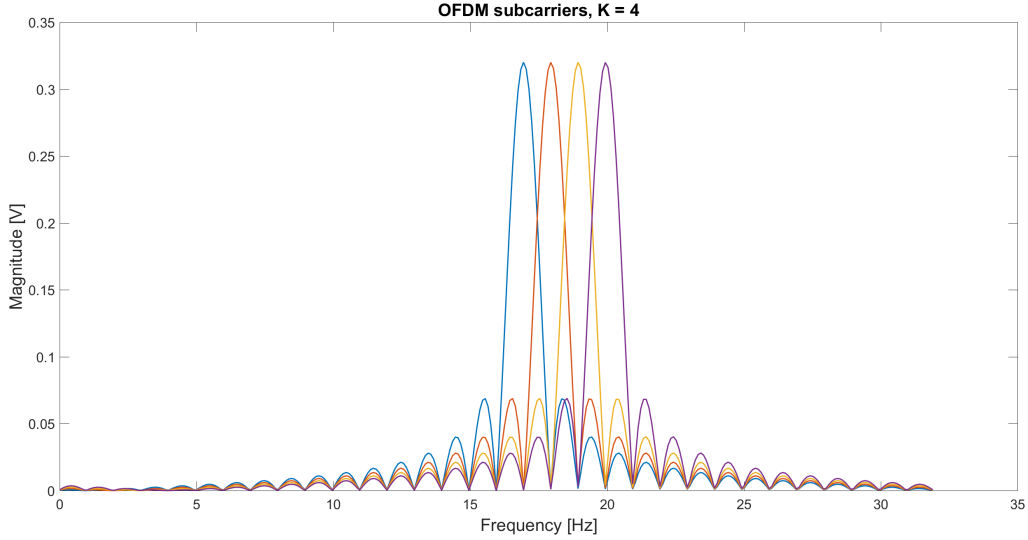


Figure 2.2: Illustration of an OFDM signal's spectrum with $K = 4$ subcarriers. The subcarriers are spaced by Δf .

2.2.2 Frequency choice and orthogonality

In OFDM, the subcarriers frequencies are chosen so that the subcarriers can be closely allocated in the frequency spectrum, their overlapping does not jeopardize the signal and a guard band is not needed. Hence, all the subcarriers must be orthogonal.

In order to achieve the subcarriers orthogonality, they must be spaced by the same frequency $\Delta f = \frac{1}{T_s}$, where T_s is the symbol duration. In this way, intercarrier interference (ICI) will not happen, as can be seen in Figure 2.2. Then, with K subcarriers, the total bandwidth will be, approximately, $W = K \cdot \Delta f$.

Since all subcarriers are orthogonal, OFDM has no need of guard bands, making it a spectral efficient scheme.

2.2.3 IDFT and DFT

The Inverse Discrete Fourier Transform (IDFT) and the Discrete Fourier Transform (DFT) are both used for modulation and demodulation on the OFDM transmitter and receiver, respectively.

Let \mathbf{X} represent the input signal for the IDFT. $\mathbf{X} = [X_0, X_1, X_2, \dots, X_{N-1}]^T$, where X_k is a signal sample in the frequency domain and will be assigned to the corresponding subcarrier with frequency f_k . \mathbf{X} is a vector with length N , where N is the IDFT size.

In addition, $\mathbf{x} = [x_0, x_1, x_2, \dots, x_{N-1}]^T$ is the corresponding time domain representative of \mathbf{X} , the output of the IDFT. \mathbf{X} represent modulated data, where Quadrature Amplitude Modulation (QAM) or Phase Shift Keying (PSK) are usually used as modulation scheme.

Below, the IDFT is presented:

$$x_m = \frac{1}{\sqrt{N}} \sum_{k=0}^{N-1} X_k \exp \frac{j2\pi km}{N}, \quad 0 \leq m \leq N-1 \quad (2.3)$$

Following, the DFT:

$$X_k = \frac{1}{\sqrt{N}} \sum_{m=0}^{N-1} x_m \exp \frac{-j2\pi km}{N}, \quad 0 \leq m \leq N-1 \quad (2.4)$$

In the transmitter, after being converted to parallel by a serial-to-parallel (S/P) converter, the IFFT acts as multiplexer and assigns each signal sample to a different subcarrier.

In the receiver, after the S/P converter, the FFT is performed on the signal, retrieving the original information out of each subcarrier.

It is important to notice that, since the baseband bandwidth of the OFDM signal is $\frac{K\Delta f}{2}$, according to the sampling theorem, the sampling frequency, f_{samp} , must obey:

$$f_{samp} = N \cdot \Delta f > K \cdot \Delta f \quad (2.5)$$

2.2.4 The cyclic prefix

Since the symbol rate is relatively slow, i.e., T_s is relatively larger than the channel impulse response, it is affordable to add a guard interval between the OFDM symbols for transmission. Instead of adding an empty guard interval between symbols, the cyclic prefix is used. In the transmitter, adding the CP to the time domain samples implies in lower bit rates but also eliminates Inter-Symbol Interference (ISI), caused by multipath propagation and ICI. The CP consists of the last samples of the OFDM symbol inserted in its beginning, in order to emulate a periodic symbol to approximate the convolution between channel and signal to an ideal circular convolution. This effect is useful in the equalization. For a better understanding, consider $\mathbf{x} = [x_0, x_1, x_2, \dots, x_{N-1}]^T$ the vector containing an OFDM signal's time domain samples. Before being transmitted, \mathbf{x} will have the CP inserted in its beginning, so that a new sequence $\mathbf{x}_{CP} = [x_{N-G}, \dots, x_{N-2}, x_{N-1}, x_0, x_1, x_2, \dots, x_{N-1}]^T$, where G is the CP length, will be produced and transmitted. In the receiver, the system removes the CP so the important information is demodulated and processed, since the CP is a redundancy [2].

2.2.5 Single Tap Equalizer

The cyclic prefix is used so any ISI due to multipath propagation may be corrected by a single tap equalizer [2].

To understand why, consider a case where there is perfect upconversion and downconversion but the received signal is the sum of two versions of the baseband transmitted signal with different gains and delays.

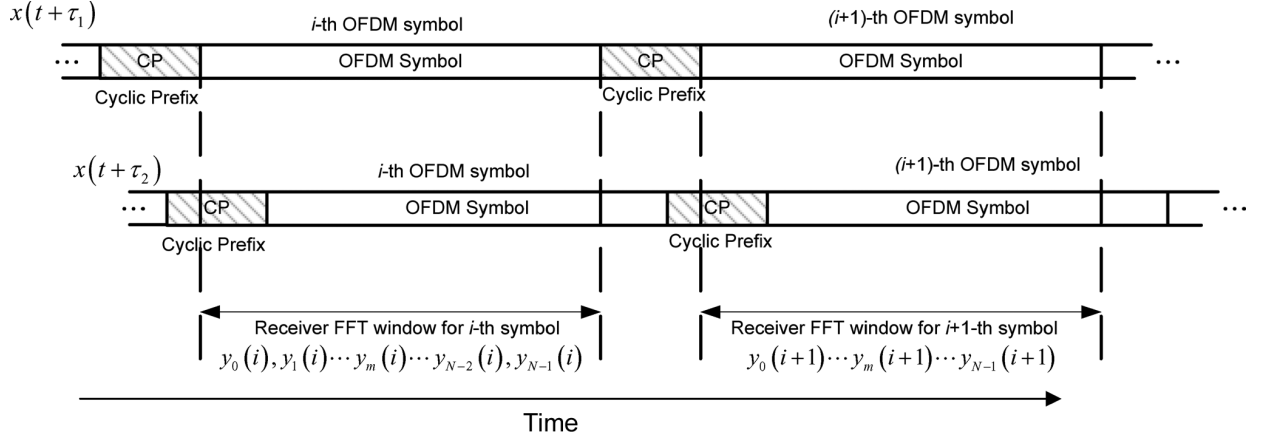


Figure 2.3: OFDM symbols in a multipath channel. Inspired by [2].

$$y(t) = g_1x(t + \tau_1) + g_2x(t + \tau_2) \quad (2.6)$$

There won't be ISI as long as the FFT window is aligned with the first symbol and the delay spread, $\tau_2 - \tau_1$, has a smaller duration than the CP's. In this way, the i -th transmitted signal depends only of the i -th transmitted symbol. This situation is illustrated at Figure 2.3.

In order to understand how the single tap equalizer is applied, consider a subcarrier in the range $0 \leq k \leq N/2 - 1$.

Let the continuous baseband signal at the transmitter, where the IDFT is performed, associated with the k -th subcarrier of an OFDM symbol be

$$x(k, t) = \frac{1}{\sqrt{N}}X_k \exp\left(\frac{j2\pi kt}{T_s}\right), \quad 0 \leq k \leq N/2 - 1 \quad (2.7)$$

Then, according to (2.6), the received signal after multipath propagation would be

$$y(k, t) = \frac{1}{\sqrt{N}}g_1X_k \exp\left(\frac{j2\pi k(t - \tau_1)}{T}\right) + \frac{1}{\sqrt{N}}g_2X_k \exp\left(\frac{j2\pi k(t - \tau_2)}{T}\right), \quad 0 \leq k \leq N/2 - 1. \quad (2.8)$$

In the receiver, since the FFT window should be aligned with the main version of the signal, the FFT window will have an offset of τ_1 . In this case,

$$y(k, t) = \frac{1}{\sqrt{N}}g_1X_k \exp\left(\frac{j2\pi kt}{T}\right) + \frac{1}{\sqrt{N}}g_2X_k \exp\left(\frac{j2\pi k(t - (\tau_2 - \tau_1))}{T}\right). \quad (2.9)$$

$$y(k, t) = \frac{1}{\sqrt{N}}X_k \exp\left(\frac{j2\pi kt}{T}\right) \times (g_1 + g_2 \exp\left(\frac{-j2\pi k(\tau_2 - \tau_1)}{T}\right)) \quad (2.10)$$

After the demodulation by the FFT and including the noise present in transmission,

$$Y_k = X_k(g_1 + g_2 \exp\left(\frac{-j2\pi k(\tau_2 - \tau_1)}{T}\right)) + W_k = H_kX_k + W_k \quad (2.11)$$

where

$$H_k = g_1 + g_2 \exp \frac{-j2\pi k(\tau_2 - \tau_1)}{T}. \quad (2.12)$$

Hence, the transmitted data may be recovered by the receiver by performing one complex multiplication, since

$$\hat{X}_k = \frac{Y_k}{H_k} = X_k + \frac{W_k}{H_k} \quad (2.13)$$

where \hat{X}_k is the estimated version of X_k .

2.2.6 Coding and Interleaving

OFDM is mostly used along with coding for error correction and interleaving.

Interleaving makes the signal more resistant to frequency selective fading by spreading the errors along the frequency spectrum or interval, so that it will be less likely for burst errors to happen and so the receiver can apply code correction. Most code correction algorithms cannot correct all errors if there is a burst of errors. So the interleaving is necessary to uniformly spread the errors, allowing a more effective performance by the error correction algorithm.

More than one layer of coding and interleaving may be used, so that small bit error rates can be achieved, even in very noisy channels.

2.2.7 Transmission and reception: D/A and A/D conversions and frequency mixing

In transmission, before being transmitted, the OFDM signal is converted to the analog domain by an D/A converter, and is frequency shifted to transmission by an I/Q modulator. For exemplification, let $x(t)$ be the output signal from the D/A and $s(t)$ be the I/Q modulator output signal. Hence, $s(t)$ is given by

$$s(t) = \Re\{x(t)\} \cos(2\pi f_c t) - \Im\{x(t)\} \sin(2\pi f_c t) \quad (2.14)$$

Where $\Re\{\cdot\}$ is the real operator and $\Im\{\cdot\}$ is the imaginary operator, $\Re\{x(t)\}$ and $\Im\{x(t)\}$ are the real and imaginary parts of $x(t)$, respectively, and f_c is the carrier frequency. For baseband signals, e.g. ADSL, $x(t)$ is a real signal. In the receiver, the signal is frequency down converted and converted to the digital domain by the A/D converter, so the other steps can be executed. For the correct frequency conversion, synchronization between transmitter and receiver is needed. This can be a disadvantage since the system out of synchronicity will cause ISI.

2.2.8 Overall Analysis

The 4G scenario is a successful application of OFDM. The scheme's main advantage are [7]:

- **Spectral efficiency:** OFDM splits the data into different orthogonal subcarriers. The orthogonality extinguishes the need of guard bands, that carry no useful information, between subcarriers, making OFDM spectrally efficient.
- **Multi-path propagation resiliency and low complexity equalizer:** The CP and symbols' long duration makes the scheme resilient to ISI caused by multi-path propagation and allows the use of a one-tap equalizer at the receiver.
- **Multiple user scheduling advantage:** OFDM's nature allow multiple users schemes, which is exploited by the multiple access scheme Orthogonal Frequency Division Multiplexing / Multiple Access (OFDMA). This scheme also makes use of time scheduling based on fixed time intervals. OFDMA is currently used in 4G.

Despite being a heavily used scheme and having many advantages, OFDM still has some drawbacks that open room for investigating other waveforms for 5G. OFDM's main disadvantages are:

- **Cyclic Prefix overhead:** The CP consists of a redundancy, it is a copy of the tail of the signal inserted in its beginning. This implies on transmission time not being used for information transmission, which is a waste of transmission rate [7].
- **Sensitivity to frequency offset:** The frequency orthogonality between subcarriers is key for OFDM functionality. In order to achieve it, receiver and transmitter must be in synchrony. If synchrony is not achieved, ICI is likely to happen.
- **Sensitivity to transmission synchronization:** In order to achieve time orthogonality between transmitted symbols, so interference between users is avoided or mitigated, all users in an OFDM system must transmit synchronously. Therefore, time advance (TA) signals are sent from the base stations to the users, in order to maintain time orthogonality in LTE networks [7].
- **High Peak-to-Average Power Ratio:** High PAPR occurs when many individual subcarriers happen to be in phase. Usually, at each instant, the subcarriers have different phases when compared to each other. However, due to the large amount of subcarriers in an OFDM symbol, occasionally, many subcarriers might simultaneously have the same phase, causing the symbol's output power to peak. This peak may lead the power amplifiers at the transceivers to saturation, implying on information loss and OOB [7].
- **Out-of-band emission:** Due to the nature of the time domain rectangular pulse, which corresponds to a sinc in frequency domain, OFDM suffers from high spectral side lobes [9].
- **Low flexibility:** In order to achieve easier to implement orthogonality, LTE utilizes a fixed set of numerology, including CP length and subcarrier spacing, across the whole system bandwidth. A flexible numerology could satisfy more heterogeneous applications since it affects performance parameters like latency, data rate and resource utilization efficiency [9].

In order to achieve a higher performance, adaptations of OFDM are investigated to compensate its weaknesses. One of the possible solutions is fOFDM, which is discussed in the following sections.

2.3 FOFDM

2.3.1 Introduction

Inspired by OFDM, filtered-OFDM seeks to maintain the original scheme's advantages, while solving some of its problems. fOFDM consists of multiple sub-bands, which are independently filtered and split among themselves. Each of the sub-bands accommodates OFDM systems.

This scheme brings some additional advantages in comparison to conventional OFDM. The sub-band-based filtering allows synchronization relaxation and asynchronous transmission of sub-bands. The filtering also provides out-of-band emission (OOBE) reduction, making it possible to reduce the guard bands between symbols, raising spectral efficiency [3]. Nowadays, LTE reserves 10% of its bandwidth as guard bands [9]. In addition, it is also possible to apply different numerology to each sub-band, providing the flexibility needed to support many heterogeneous applications [3].

Since fOFDM keeps many of OFDM's original features, the transition from 4G LTE to 5G would be smooth.

2.3.2 Flexibility

5G will deal with diverse applications and OFDM alone will not be able to provide the necessary flexibility.

OFDM operates with a fixed time-frequency grid, where symbols have fixed transmission time interval (TTI) and subcarrier spacing. Moreover, it demands extensive signaling in order to achieve synchronization and, consequently, orthogonalization between symbols. When orthogonalization is not available, OFDM suffers extensive performance degrading.

FOFDM is designed to provide the flexibility to support numerous diverse applications. In this scheme, the bandwidth is split into several sub-bands, as illustrated by Figure 2.4. In each sub-band, a conventional OFDM, or another waveform, is set to fit the application needs or channel characteristics, with suitable subcarrier spacing, cyclic prefix length and TTI [3, 14, 15]. In addition, flexibility may be used to improve the system performance according to channel conditions.

Sub-band filtering is performed in order to suppress inter-sub-band interference. Filtering an OFDM signal presents a drawback, which is breaking the time orthogonality between OFDM symbols. The filtering operation elongates the symbol in time domain, thus causing intersymbol interference (ISI). However, with proper filter design, it is possible to mitigate ISI effects. Hence, a lower OOBE is achieved with little ISI, so the guard band between different sub-bands can be reduced to small tones or no guard band at all [3]. These guard tones may be as small as the chosen subcarrier spacing, or even smaller. Therefore, the fOFDM systems provide better spectral

efficiency in comparison with traditional OFDM systems, since the latter allocates around 10% of the available bandwidth as guard band.

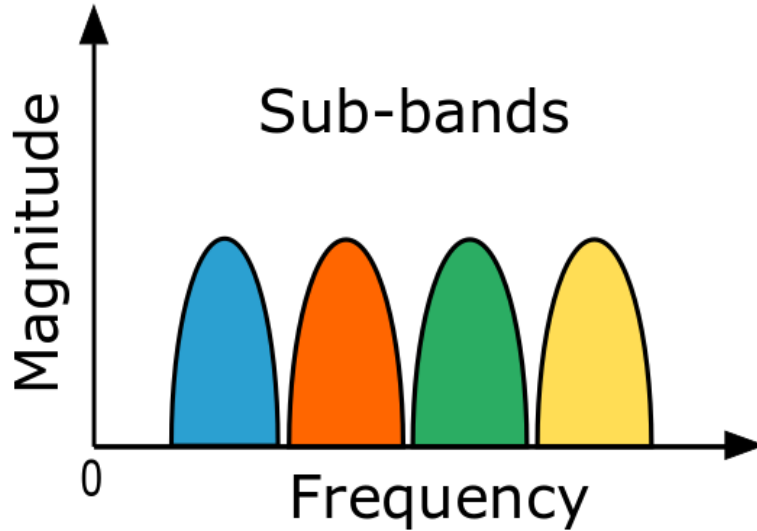


Figure 2.4: Illustration of a spectrum division into sub-bands.

In conclusion, fOFDM’s flexibility is enabled by its sub-band filtering and its low OOB.

fOFDM resource allocation is illustrated by Figure 2.5. As can be seen, the resource blocks are flexibly allocated. For instance, to provide ultra-low latency and highly reliable vehicle-to-vehicle communication, the TTI is shortened while subcarrier spacing is increased, augmenting speed and reliability, respectively.

For IoT, a sub-band may be allocated for a single-carrier scheme access, with small bandwidth and long TTI, in order to assist low power consumption devices. These are just some examples of what fOFDM flexibility provides.

2.3.3 Transceiver Structure

The fOFDM transceiver is exhibited in Figure 2.6.

Different OFDM systems with different numerology are assigned to different sub-bands. Usually, the sub-bands do not interfere with each other and are separated by guard tones, much smaller than LTE’s guard bands, making asynchronous transmission possible between different sub-bands.

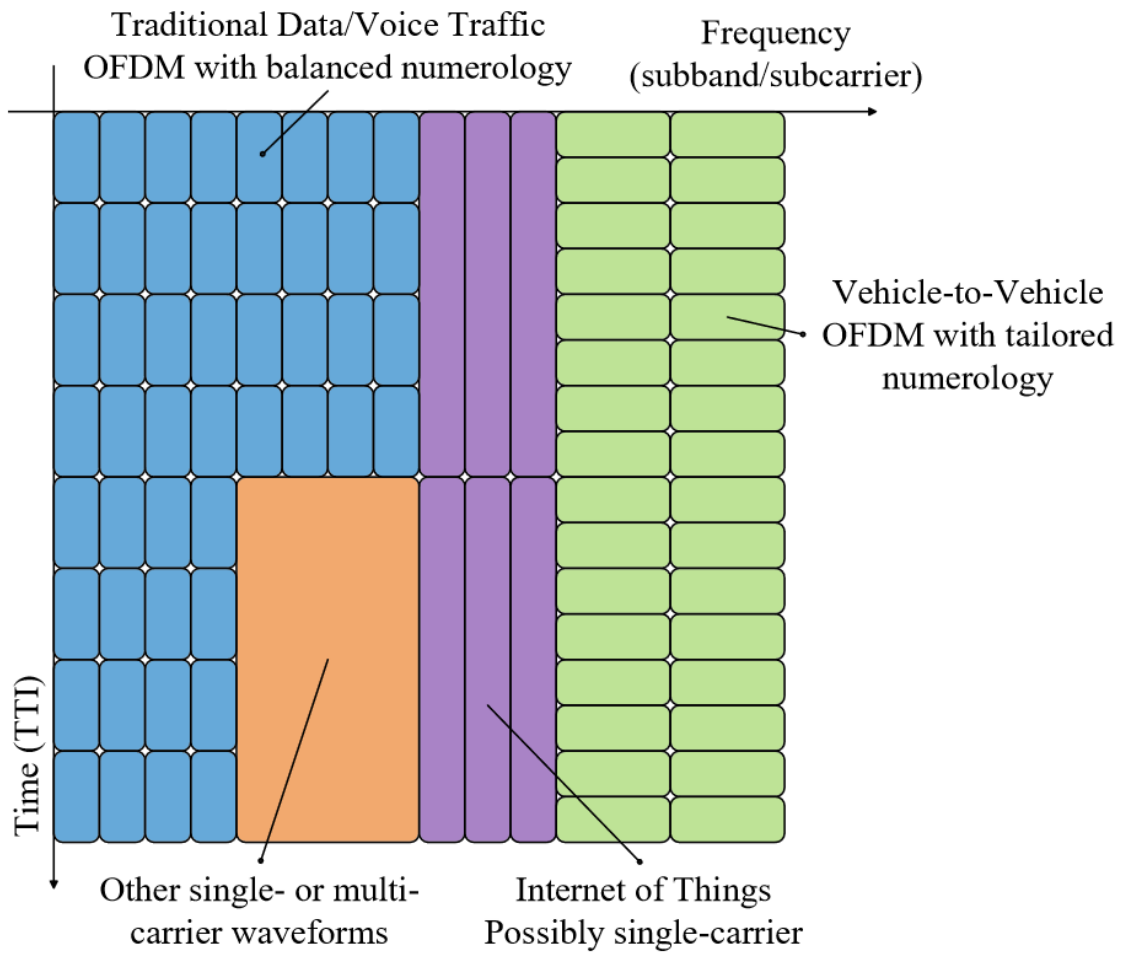


Figure 2.5: FOFDM resource allocation. Extracted from [3].

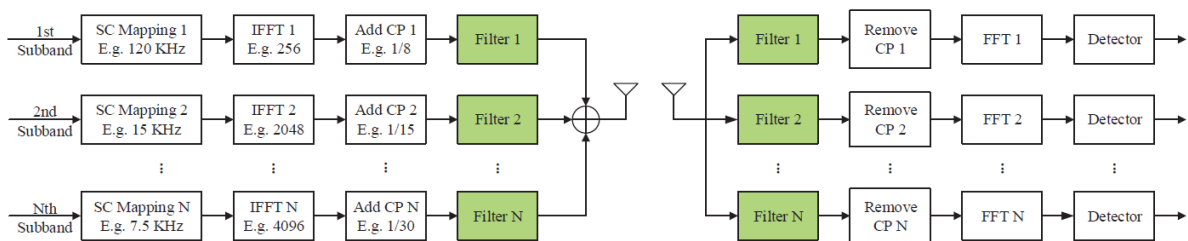


Figure 2.6: Downlink transceiver structure of fOFDM. Extracted from [3].

2.3.4 Filter Design and Implementation

In order to obtain sub-band filtering and take advantage of OFDM benefits, proper filter design is needed. The filter must deal with the OOB in order to constrain ICI and also have a sharp transition in the frequency domain.

However, the sharper the filtering is in frequency domain, the more elongated the filtered signal will be in time domain. Hence, there is a time-frequency trade-off when filter design is concerned.

Additionally, a real-time filter generation scheme is desirable in order to obtain flexible sub-band allocation.

Throughout this text, FIR filters were used in the fOFDM scheme. Their design is fast and simple, suitable for real-time filter generation.

In chapter 3, filter design is discussed in more depth.

Chapter 3

FIR Filters

Since fOFDM requires real-time filter generation, FIR filters are strong candidates as fOFDM filters, due to their simple design and implementation, which will be verified throughout the chapter. In addition, their impulse response does not present stability problems.

There are numerous designing methods for FIR filters. In this text, the simplest one is used, which is the window method.

3.1 Causal Filters

Ideal filters are impossible to realize because they are not causal. In order to obtain a response similar to an ideal filter's, one option is to truncate the ideal filter, obtaining a causal response [16].

Let's take, as an example, the classic brick wall (low pass) filter in Figure 3.1.

The ideal low pass filter is modeled as a rectangular pulse function $\frac{1}{B}rect(\frac{\omega}{2\pi B})$, where $2B$ is the filter width in the frequency domain and ω is the continue frequency. The filter impulse response is given by its inverse Fourier Transform (3.1)

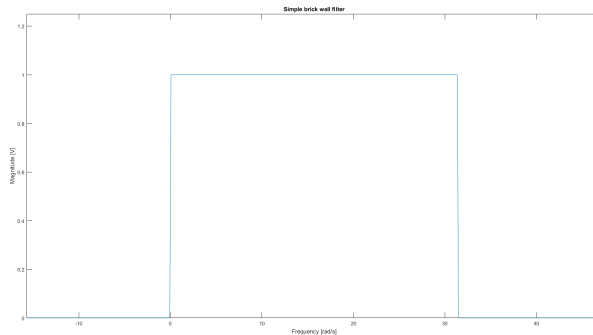


Figure 3.1: Simple brick wall filter.

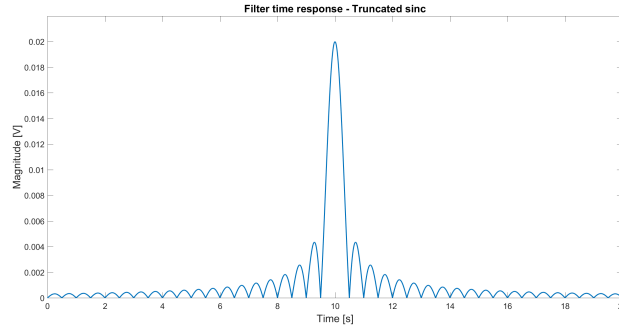


Figure 3.2: Truncated sinc.

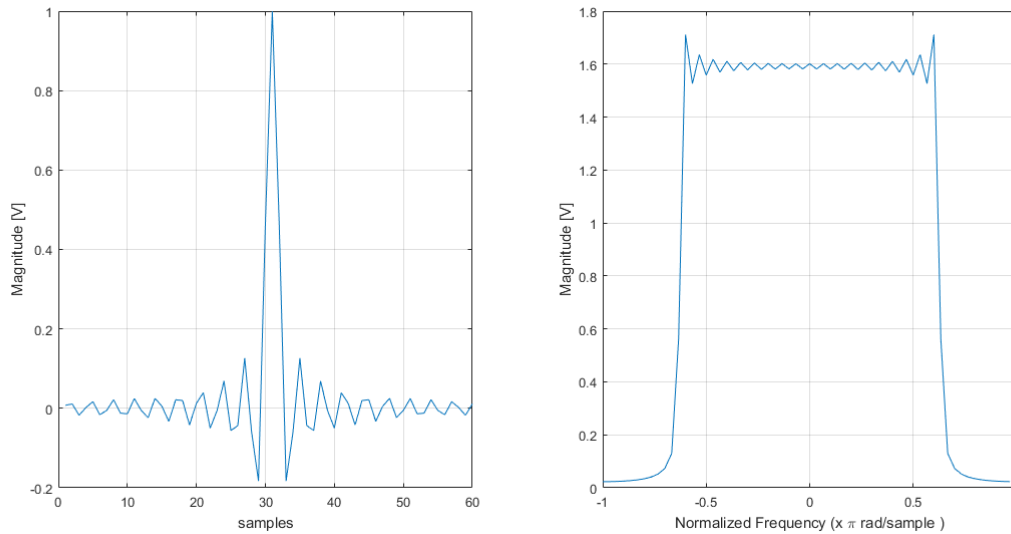


Figure 3.3: Shorter truncated sinc generating a lesser quality filter.

$$\text{sinc}(\pi Bt) \xrightarrow{\mathcal{F}} \frac{1}{B} \text{rect}\left(\frac{\omega}{2\pi B}\right). \quad (3.1)$$

The ideal low pass filter has an infinite impulse response, which is a sinc function, making it impossible to realize this filter. However, it is possible to truncate the ideal impulse response in order to obtain an impulse response close to the non-causal case, as show in Figure 3.2.

The longer the truncated sinc, the closer the impulse response will be to the ideal one. However, the response's fidelity comes with a computational trade-off. Hence, it is necessary to find the balance between fidelity and required computational power, which will vary according to the filter's application. The effect caused by the length of the truncated sinc is pictured in Figures 3.3 and 3.4. It is visible that, the longer the truncated impulse response, the more the filter frequency response resembles an ideal one. The filter edges become sharper and the ripple oscillations become smaller at pass-band.

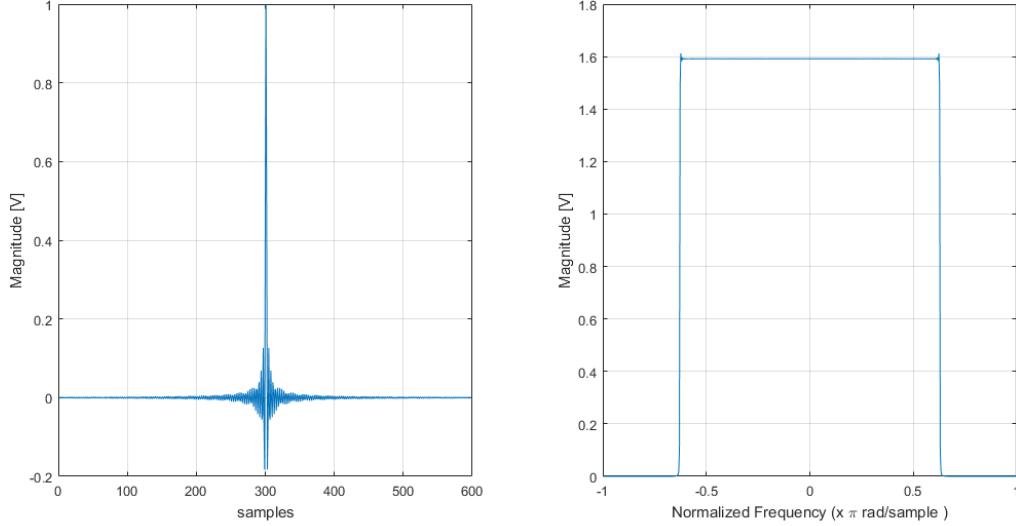


Figure 3.4: Longer truncated sinc generating a higher quality filter.

3.2 The Window Method

In order to design a digital filter, first we begin with the desired frequency response $H_d[\Omega]$ and determine the corresponding unit sample response $h_d[n]$ [16], where Ω is the discrete frequency domain in *rad/sample*, $H_d[\Omega]$ and $h_d[n]$ are discrete. Both responses are related by the Fourier transform, (3.2),

$$h_d[n] \xrightarrow{\mathcal{F}} H_d[\Omega]. \quad (3.2)$$

In general, the desired response $h_d[n]$ will have an infinite duration and must be truncated at some point $M - 1$, so the FIR Filter will have a finite length M . The truncation is equivalent to multiplying $h_d[n]$ by a window $w[n]$. Let us take the rectangular window (3.3) as an example.

$$w[n] = \begin{cases} 1, & n = 0, 1, \dots, M-1 \\ 0, & \text{otherwise} \end{cases} \quad (3.3)$$

The multiplication $h_d[n] \times w[n]$ yields,

$$h[n] = h_d[n]w[n] = \begin{cases} h_d[n], & n = 0, 1, \dots, M-1. \\ 0, & \text{otherwise.} \end{cases} \quad (3.4)$$

where $h[n]$ is the resulting FIR filter.

In the frequency domain, the window will also exert its effects. Since there was a multiplication in time, there will also be a convolution in frequency. Consider the window's DFT

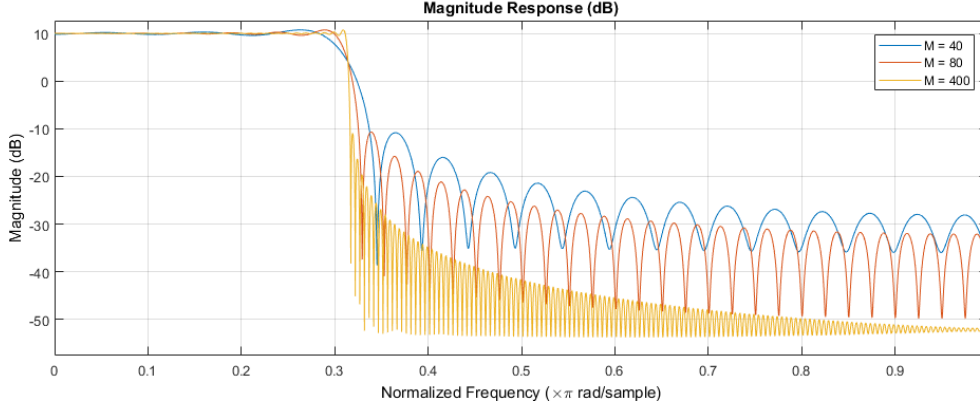


Figure 3.5: Window's size effects on magnitude response.

$$W[\Omega] = \sum_{k=0}^{M-1} w[n] e^{-j\Omega_k n}, \Omega_k = 2\pi \frac{k}{M}. \quad (3.5)$$

Hence, the convolution between $H_d[\Omega]$ and $W[\Omega]$ will be

$$H(\Omega) = H_d[\Omega] \otimes W[\Omega] = \frac{1}{2\pi} \int_{-\pi}^{\pi} H_d(v) W(\Omega - v) dv. \quad (3.6)$$

In our example, where $w[n]$ is a rectangular window, $W[\Omega]$ is

$$W[\Omega] = e^{-j\Omega(M-1)/2} \frac{\sin(\Omega(M-1)/2)}{\sin(\Omega/2)} \quad (3.7)$$

The window function has a magnitude response

$$|W[\Omega]| = \left| \frac{\sin(\Omega M/2)}{\sin(\Omega/2)} \right|, \quad (3.8)$$

and a piecewise linear phase

$$\Theta(\Omega) = \begin{cases} -\Omega(\frac{M-1}{2}), & \sin(\Omega M/2) \geq 0 \\ -\Omega(\frac{M-1}{2}) + \pi, & \sin(\Omega M/2) < 0 \end{cases} \quad (3.9)$$

The window's magnitude response is portrayed in figure 3.5, for $M = 40, 80$ and 400 . It is perceptible that the increase of M causes a decrease in the response's main lobe width, and also a decrease in the side lobes magnitude and width.

The costs of using a larger M are the required computational power and the filtered signal time elongation, which may cause ISI.

The window's characteristics play a significant role in determining the resulting frequency response of FIR Filter, obtained by truncating $h_d[n]$ to length M . The convolution of $H[\Omega]$ with

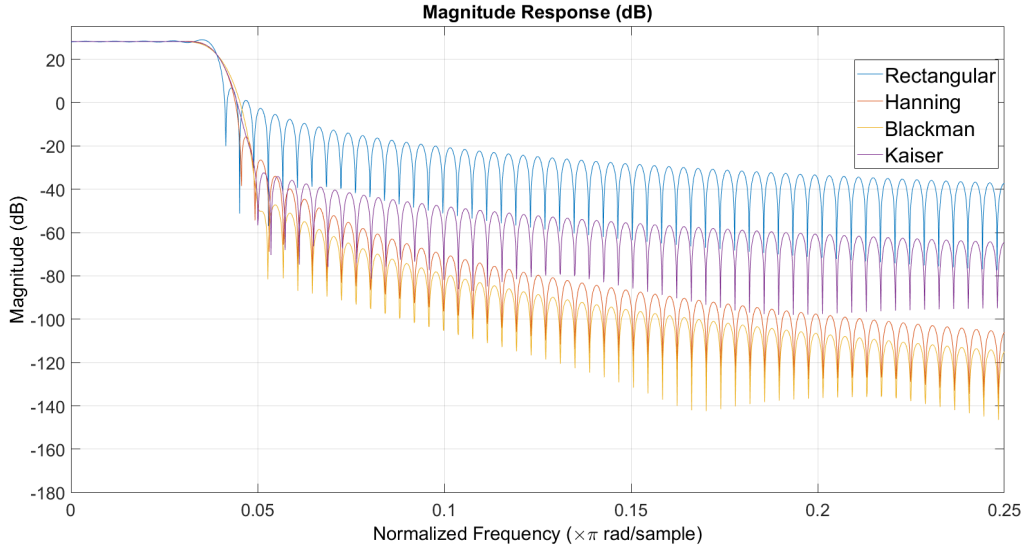


Figure 3.6: FIR filter's magnitude response with different windows.

$W[\Omega]$ has the effect of smoothing $H_d[\Omega]$. As M increases, $W[\Omega]$ becomes sharper. In order to alter how the main and side lobes reacts to the windowing process, it is possible to choose other windows besides the rectangular. Some of these windows are defined next.

Hanning	$0.54 - 0.46 \cos\left(\frac{2\pi n}{M-1}\right)$
Blackman	$0.42 - 0.5 \cos\left(\frac{2\pi n}{M-1}\right) + 0.08 \cos\left(\frac{4\pi n}{M-1}\right)$
Kaiser	$\frac{I_0[\alpha\sqrt{(\frac{M-1}{2})^2 - (n - \frac{M-1}{2})^2}]}{I_0[\alpha(\frac{M-1}{2})]}$

It is also important to observe how the side lobes behaves according to the chosen window. As presented in figures 3.6 and 3.7, the rectangular window has the smallest main lobe in magnitude response, providing a narrower transition band than other windows, but also presenting the smaller side lobes decay along with the smallest decay in impulse response, which may cause ICI and ISI, respectively.

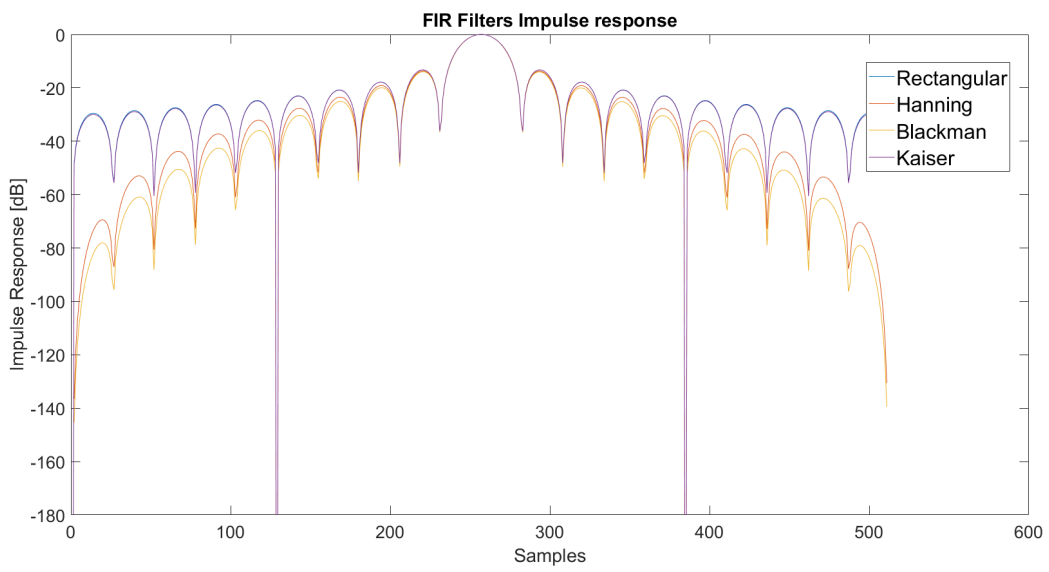


Figure 3.7: FIR filter's impulse response with different windows.

Chapter 4

The HERMES Simulator

The goal of this text is to present fOFDM simulations results in some diverse scenarios. All the simulations were performed by the Heterogeneous Radio Mobile Simulator (HERMES), which is an open-source link simulator for 4G and 5G networks [17].

4.1 About HERMES

HERMES is a link-level communications simulator designed for studying the physical layer of 4G and 5G communications systems.

It is written in MATLAB language and it has already been used in other works beyond this text [18]. In order to achieve a deeper understanding about HERMES, the reader is invited to check the simulator's code, which is available at [17].

HERMES is flexible and customizable, allowing simulations of multiple nodes communicating, synchronously or asynchronously.

There is also the possibility of simulating multiple waveforms such as OFDM, fOFDM, FBMC, and others, in different channels and with different multipath models such as the standard COST-259.

Different types of error correction codes are already implemented. Some of them are the much used turbo coding and convolutional coding.

HERMES allows a high control over the simulations, allowing the user to decide over the simulated technologies, channel model, modulations and code rates, noise, frame structure and other parameters [18, 19]. When needed, the user may implement new features with straight MATLAB programming.

In order to perform the investigations proposed in this text, the author implemented different filtering windows for the FIR filters used throughout the text, complementing the previous work done in [18].

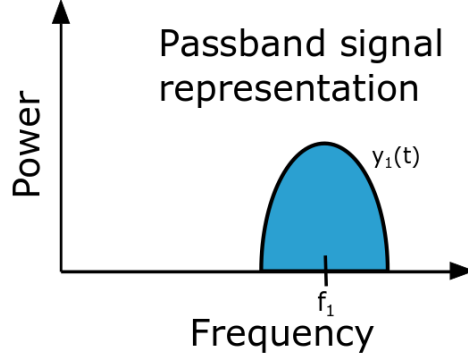


Figure 4.1: Illustration of signal $y_1(t)$.

4.2 Sampling

HERMES works with the simulated signal baseband-complex envelope, in order to minimize the sampling rates, thus decreasing the simulation runtime.

The simulator supports multiple signals transmissions, with different carrier frequencies, so their interference may be studied, which is essential for 5G investigations.

4.2.1 Single signal transmission

Take a signal $x_1(t)$, with bandwidth B_1 , that will be transmitted in a high carrier frequency f_1 with a changing phase $\theta_1(t)$, as illustrated by 4.1. The frequency mixed signal will then be

$$y_1(t) = x_1(t) \cos(2\pi f_1 t + \theta_1(t)). \quad (4.1)$$

In order to perform digital signal processing over the modulated signal, the signal would be sampled in a sampling rate f_{s1} greater than the Nyquist rate, i.e.

$$f_{s1} \geq 2 \times \left(f_1 + \frac{B_1}{2}\right), \quad (4.2)$$

according to [16]. Most of the time, this sampling process is impracticable for commonly used frequencies.

One way to simulate a single signal transmission and reception in a more efficient way is to represent the passband signal in baseband representation, in order to simulate the whole communication process in baseband.

Take our passband signal, $y_1(t)$. We can represent $y_1(t)$, which is a real signal, as a function of its quadrature components [20]:

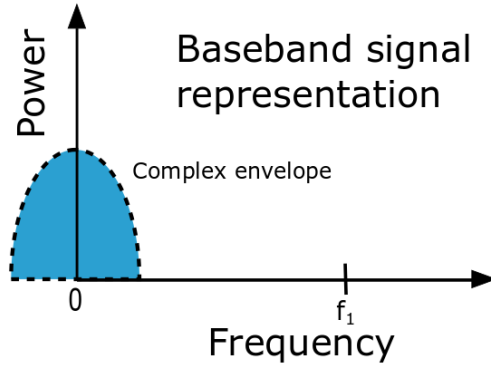


Figure 4.2: Complex envelope of $y_1(t)$.

$$y(t) = y_{1I}(t) \cos(2\pi f_1 t) - y_{1Q}(t) \sin(2\pi f_1 t), \quad (4.3)$$

where $y_{1I}(t)$ and $y_{1Q}(t)$ are the in-phase and in-quadrature components, respectively.

$$y_{1I}(t) = x_1(t) \cos(\theta_1(t)) \quad (4.4)$$

$$y_{1Q}(t) = x_1(t) \sin(\theta_1(t)) \quad (4.5)$$

$y_1(t)$'s complex envelope $\tilde{y}_1(t)$ will be

$$\tilde{y}_1(t) = y_{1I}(t) + jy_{1Q}(t), \quad (4.6)$$

which is a complex baseband signal that fully represents the original passband signal, as portrayed by figure 4.2.

The transmitted information signal $x_1(t)$ and the transmitted signal phase $\theta_1(t)$ are fully recoverable since

$$y_1(t) = \Re\{\tilde{y}_1(t)e^{j2\pi f_1 t}\}, \quad (4.7)$$

$$x_1(t) = \sqrt{y_{1I}^2(t) + y_{1Q}^2(t)} \quad (4.8)$$

and

$$\theta_1(t) = \tan^{-1} \frac{y_{1Q}(t)}{y_{1I}(t)}, \quad (4.9)$$

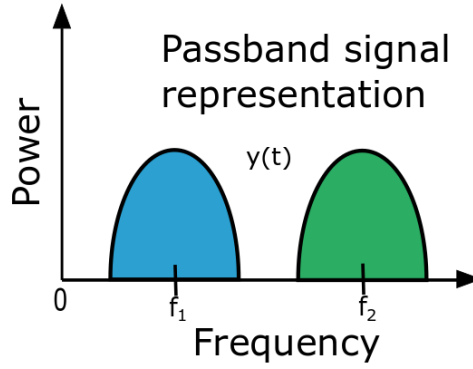


Figure 4.3: Passband representation of $y(t)$.

where $\Re\{\cdot\}$ is the real operator.

By working with a baseband signal, the simulation process becomes much computational cheaper than working with a passband signal, since the required sampling will be much smaller.

By simulating a baseband communication, the sampling frequency will be

$$f_s \geq 2 \times \frac{B_1}{2} = B_1, \quad (4.10)$$

so f_s is allowed to be much smaller than f_{s1} .

4.2.2 Multiple signals transmission

When simulating multiple signals transmission, it is also possible to use the strategy presented in the previous section. As an example, take a second signal, $x_2(t)$, that will be transmitted in a central frequency $f_2 > f_1$, with bandwidth B_2 . As illustrated by figure 4.3, the frequency mixed signal would be

$$y_2(t) = x_2(t)\cos(2\pi f_2 t + \theta_2(t)). \quad (4.11)$$

However, since $x_1(t)$ and $x_2(t)$ will be transmitted simultaneously, the resulting signal will be

$$y(t) = y_1(t) + y_2(t) = x_1(t)\cos(2\pi f_1 t + \theta_1(t)) + x_2(t)\cos(2\pi f_2 t + \theta_2(t)). \quad (4.12)$$

In order to perform digital signal processing over $y(t)$, since $f_2 > f_1 + \frac{B_1}{2} + \frac{B_2}{2}$, the signal $y(t)$ must be sampled in a sampling rate f_{s2} , where

$$f_{s2} \geq 2 \times (f_2 + \frac{B_2}{2}). \quad (4.13)$$

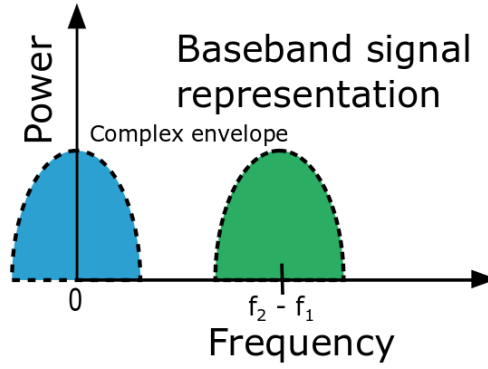


Figure 4.4: Baseband representation of $y(t)$.

Therefore, depending on f_2 and B_2 , the sampling process may become very computational costly.

To achieve a lower sampling rate f_s , for simulation purposes, make the signal with the lowest carrier frequency a baseband signal (complex envelope), in this case $y_1(t)$. Next, the other signals, in this case only $y_2(t)$, are negatively offset in the spectrum by the baseband signal's central frequency, f_1 , as show by figure 4.4.

Now, since $f_2 > f_1$, the new sampling rate f_s is

$$f_s = 2 \times (f_2 - f_1 + \frac{B_2}{2}). \quad (4.14)$$

Hence, the new sampling rate f_s is allowed to be much smaller than f_{s2} , by a factor of $2 \times f_1$.

If there is more than two signals, the process may be replicated without loss of generality.

HERMES' main feature is its flexibility, that enables multiple signals simulations. It is designed to deal with signals that have different carrier frequencies, sampling rates and are asynchronously transmitted.

All signals simulated by HERMES are generated as baseband signals.

In order to deal with diverse signals, HERMES compares the signals' sampling rates and upsamples all transmitted signals to the higher sample rate. Next, it shifts the signals to their respective carrier frequencies. The signals are added and the resulting signal is downsampled to the receiver frequency, forming the received signal.

4.3 Frame structure

HERMES allows the user to fully customize the transmitted signal frame structure.

Throughout this work, the used frame structure consists of downlink and uplink control over-

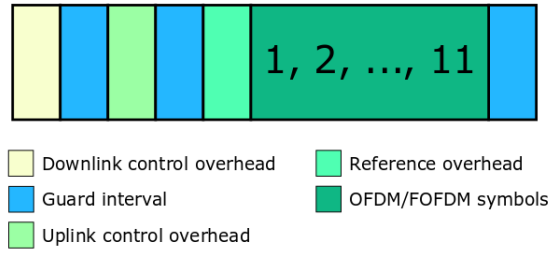


Figure 4.5: Frame structure illustration.

heads, guard intervals, reference overhead, and 11 OFDM or fOFDM symbols, distributed as illustrated by Figure 4.5.

This frame structure was chosen in order to follow 5G principles [21].

Chapter 5

Simulation Results

Computational simulations allow testing concepts without the need of experimentation and also the investigation of problems that cannot be analytically described. They are much cheaper and provide faster results than field testing, which makes them very attractive to engineering and science in general.

In this text, the fOFDM waveform is studied and compared with its predecessor, OFDM, so its benefits, features and viability as a 5G waveform may be verified. All the investigations and studies were performed by the HERMES simulator.

In the next sections, the results of diverse simulated scenarios as well as the obtained conclusions are presented and discussed.

5.1 Filter design impact on fOFDM performance

Throughout this section, the analyzed signals were generated according to the parameters in Table 5.1.

All of fOFDM advantages over OFDM are achieved as consequence of filtering the transmitted signal. Therefore, the filter design plays a big role at fOFDM performance. In this section, different analysis are made in order to understand how the communication signal behaves with different FIR

Table 5.1: Parameters table.

Parameters	Value/Description
FFT size	512
Useful subcarriers	400
Subcarriers spacing	15kHz
User speed	36km/h
Modulation	QPSK
Cyclic Prefix length	$(1/8)512 = 64$

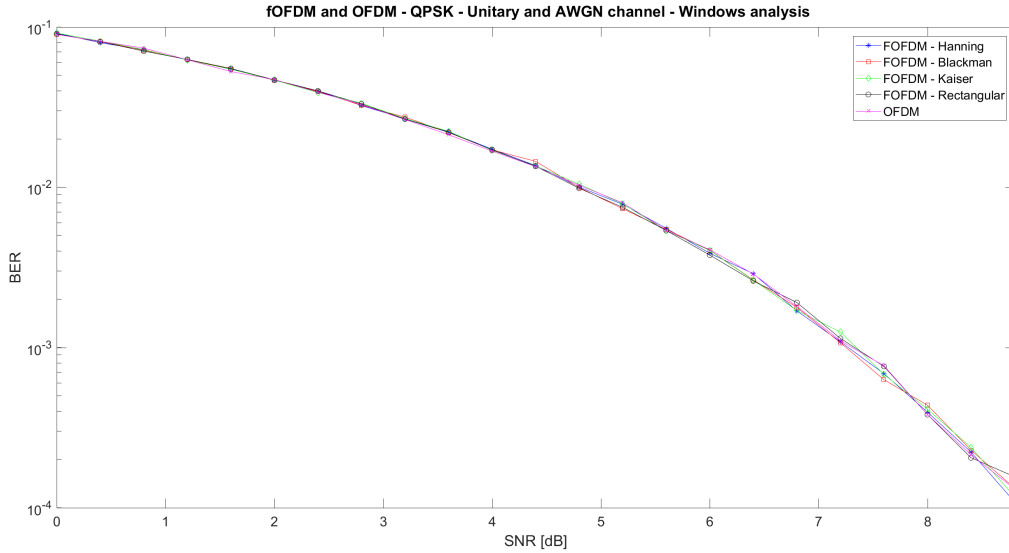


Figure 5.1: BER obtained by simulating the transmission of fOFDM, with different filters, and OFDM symbols.

filters.

5.1.1 Window impact on fOFDM performance

One of the desired features of fOFDM is sub-band filtering. It provides the spectrum division into sub-bands with independent numerology. Therefore, applications with different requirements will be assigned to the sub-bands that satisfy the required symbol size, modulation, latency, resiliency, and so forth.

The sub-bands are filtered in order to mitigate the effects caused by their mutual interference, which brings the attention to the studying of filters.

In this work, FIR filters were investigated. Due to their simplicity, it is possible that this category of filters will become standard [22]. The design was made by applying the window method. Hence, it is of interest to study how the window affects the scheme's performance.

For a no-interfering scenario, AWGN channel with no multipath, Figure 5.1 shows that fOFDM and OFDM provide similar performances. In addition, the chosen window will not affect fOFDM's performance in these conditions.

Next, the simulation consists of two signals in adjacent bands. When the interference-to-signal ratio (ISR) is 0dB, and the transmission is synchronous, fOFDM and OFDM perform similarly, as shown by Figure 5.2.

By lifting the ISR to 10dB, some differences begin to appear. Figure 5.3 portrays that fOFDM's BER is slightly affected by the used window. In this simulation, the rectangular window achieved a slightly poorer performance, while OFDM was the best scheme.

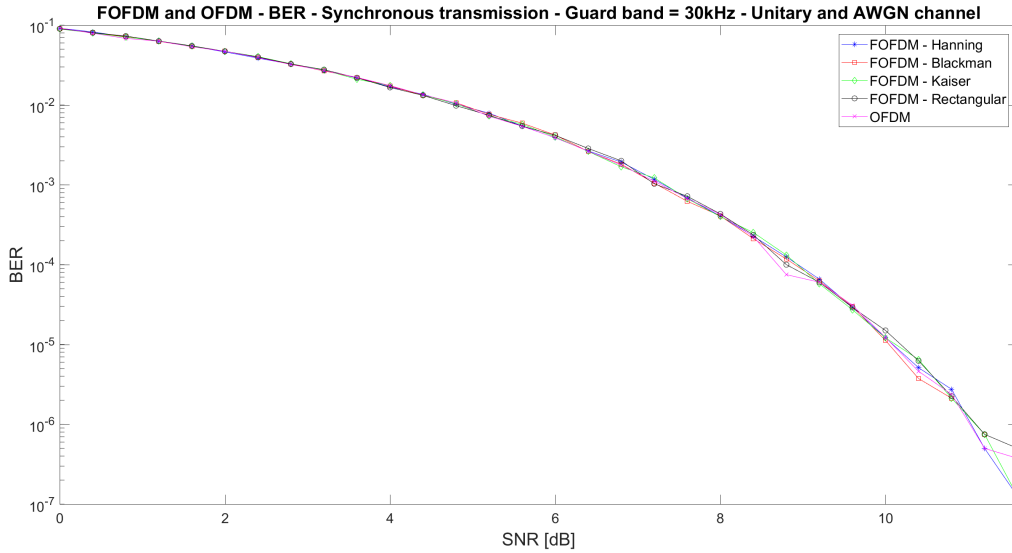


Figure 5.2: BER obtained by simulating the transmission of fOFDM, with different filters, and OFDM symbols. Each simulation run was composed of two signals with the same technology and a frequency separation of 30 kHz.

Another interesting scenario is the asynchronous transmission. When synchronization between symbols is lost, OFDM loses its time orthogonality. That is when fOFDM shines. This situation is better explained later in this chapter.

Figure 5.4 shows how fOFDM stands out in an asynchronous transmission. FOFDM's BER was considerably smaller than OFDM's. All windows had similar BER curves, while regular OFDM had a considerable performance degrading.

A good performance, by fOFDM, in asynchronous transmission is desired, since it is necessary for the numerology flexibility between sub-bands.

5.1.2 Filter order effects

One of fOFDM qualities is its low OOB. This effect is achieved thanks to the filtering the fOFDM signal goes through.

Figure 5.5 presents how the spectrum differs between OFDM and fOFDM schemes.

FOFDM's frequency characteristics can be controlled by modifying the FIR filter's order and the filter window. As the order is increased, the filtered signal becomes shorter in frequency. However, large increases in the filter order achieve only small improvements in frequency characteristics, beyond requiring more computational power. In Figures 5.6 and 5.7, the signal spectrum is exhibited for different filter orders.

On account of fOFDM being expected to be used in asynchronous transmissions, it is of interest to study how the filter order directly affects the scheme's BER curve.

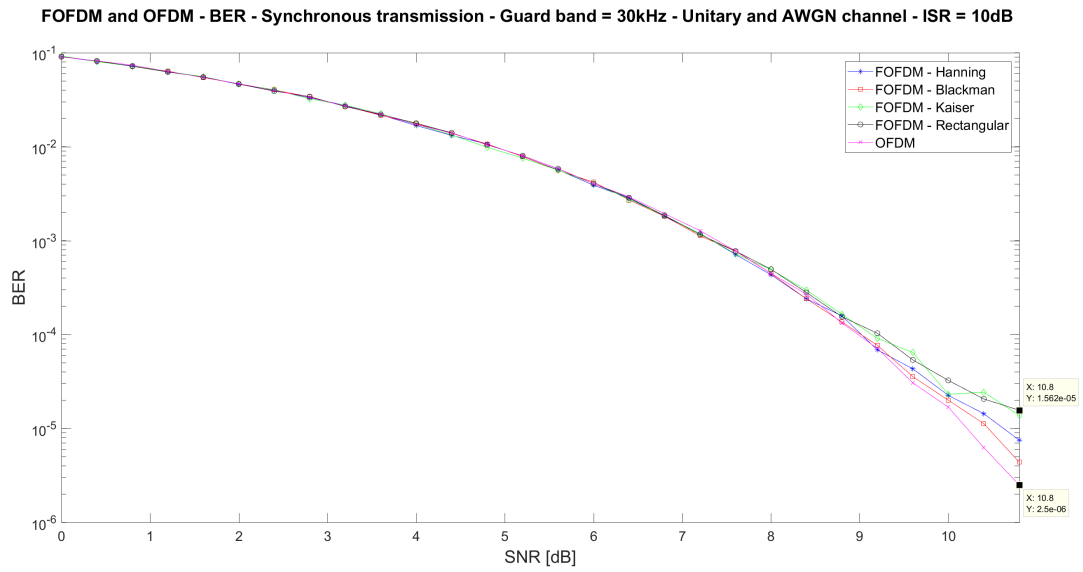


Figure 5.3: FOFDM and OFDM in synchronous transmission. ISR = 10dB.

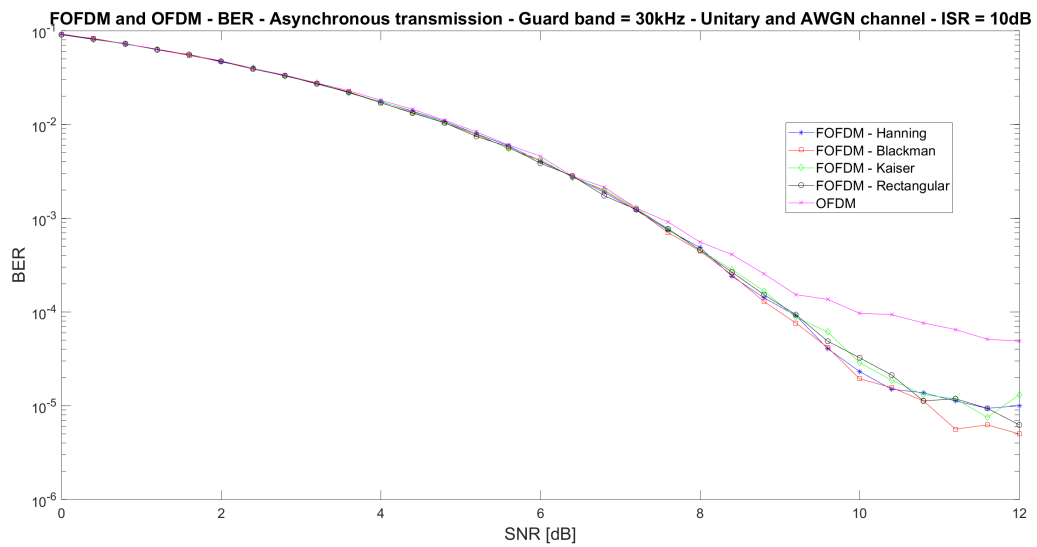


Figure 5.4: FOFDM and OFDM in asynchronous transmission. ISR = 10dB.

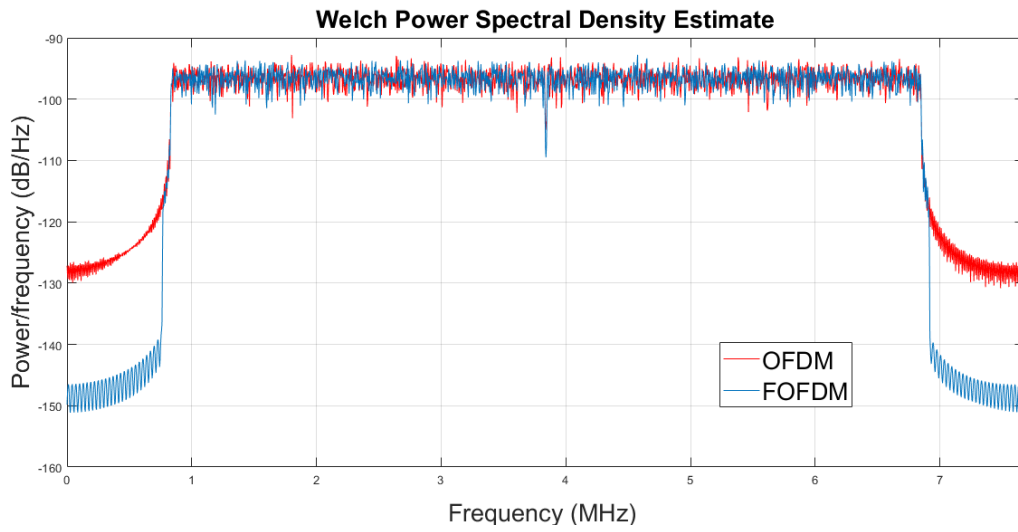


Figure 5.5: Comparison between fOFDM and OFDM signals in the frequency domain. In this case, fOFDM's OOB level was 20dB lower than OFDM's.



Figure 5.6: Comparison between two fOFDM signals in the frequency domain with different filter orders. Notice how the spectrum decay is faster for the higher order filter.

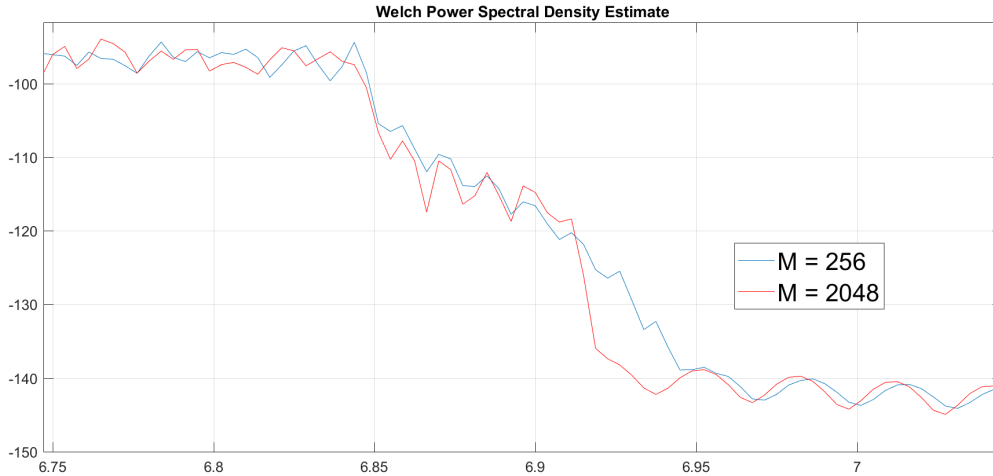


Figure 5.7: Zooming over the spectrum decays presented in Figure 5.6, so the reader may take a better look over the differences between the signals.

When the filter order is increased, the filter becomes sharper in the frequency domain and its OOB is also decreased. On the other hand, in time domain, the filtered signal will be larger than the original signal, which raises ISI.

By simulating transmissions, according to the parameters on Table 5.2, it can be verified, at Figures 5.8 and 5.9, that increasing the filter order actually degrades the system's performance by a small amount.

Even though increasing the filter order may seem good at first hand, it actually generates a considerable amount of ISI that raises the BER when compared to lower-order filters.

Doubling the CP length will mitigate the ISI caused by the filter, which makes different filter orders deliver similar results, as can be seen in Figure 5.10. However, increasing CP length is usually undesirable, since it implies in inefficient use of resources.

Therefore, increasing the filter order is not desired. Beyond degrading the BER, for a given CP length, it also increases computational cost for the filtering process, proportionally to the filter order.

However, the filter order may also not be indefinitely diminished, since it will alter significantly the filter characteristics such as cutoff frequency and sharpness, as can be seen in Figure 5.11. When the filter order is too low, the BER curve will be heavily affected, as displayed on Figure 5.8.

5.2 Multipath propagation

Multipath propagation is a phenomenon that may degrade transmission when not dealt with.

In the latest years, OFDM has elegantly dealt with multipath propagation by making use of

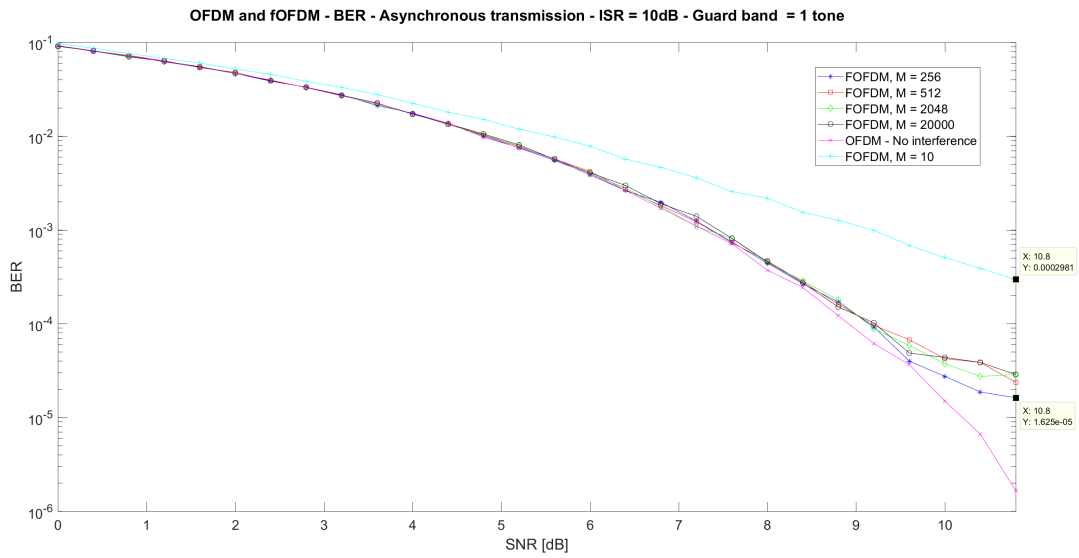


Figure 5.8: FOFDM's performance under asynchronous transmission. ISR and guard band are fixed while the filter order M is varied.

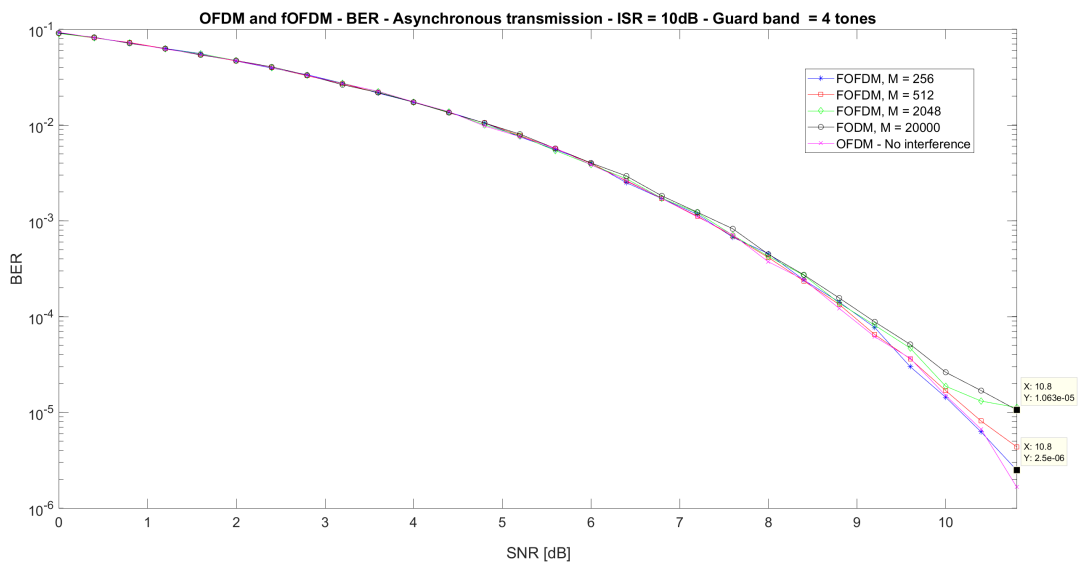


Figure 5.9: FOFDM's performance under asynchronous transmission. ISR and guard band are fixed while the filter order M is varied.

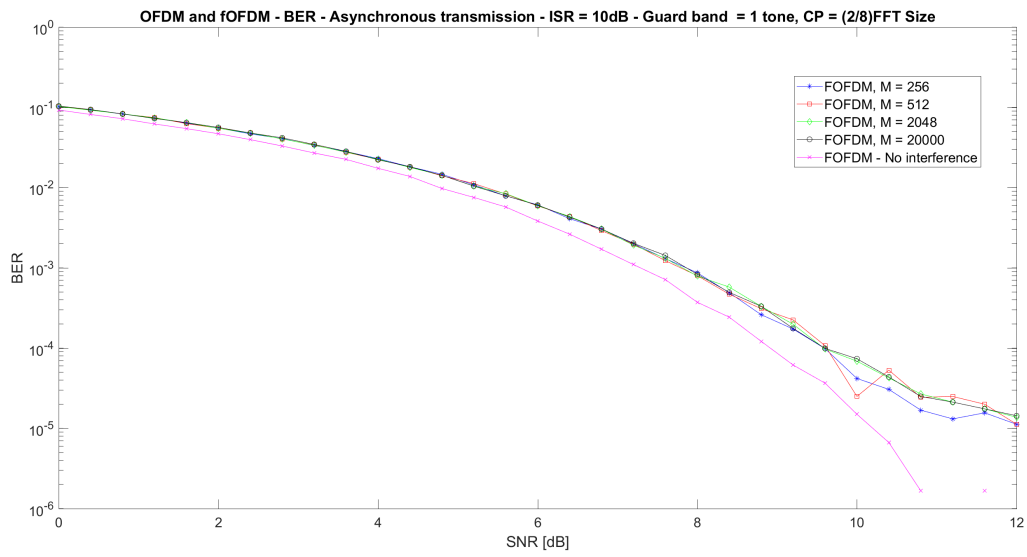


Figure 5.10: FOFDM's performance under asynchronous transmission. ISR and guard band are fixed while the filter order M is varied, with a doubled CP length.

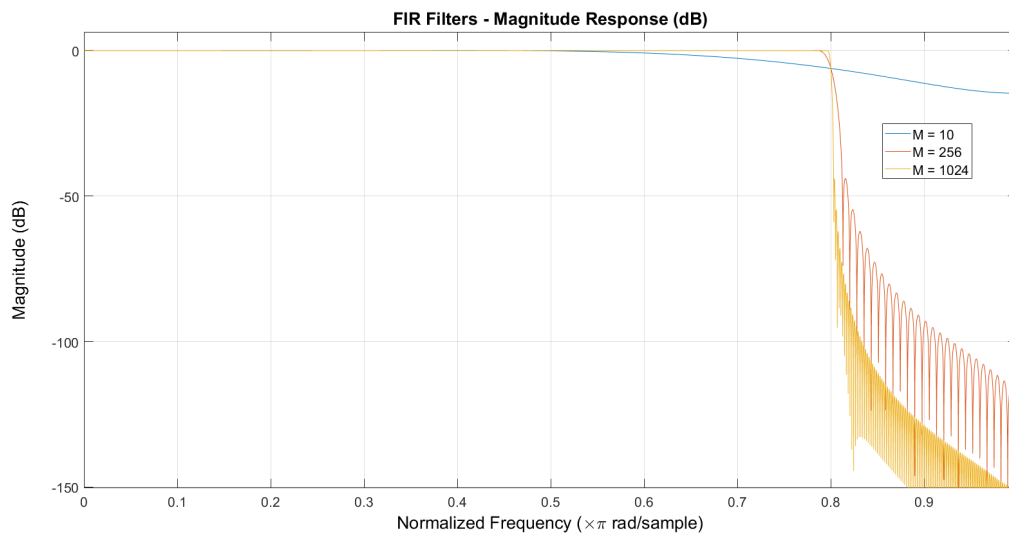


Figure 5.11: FIR filter with different orders.

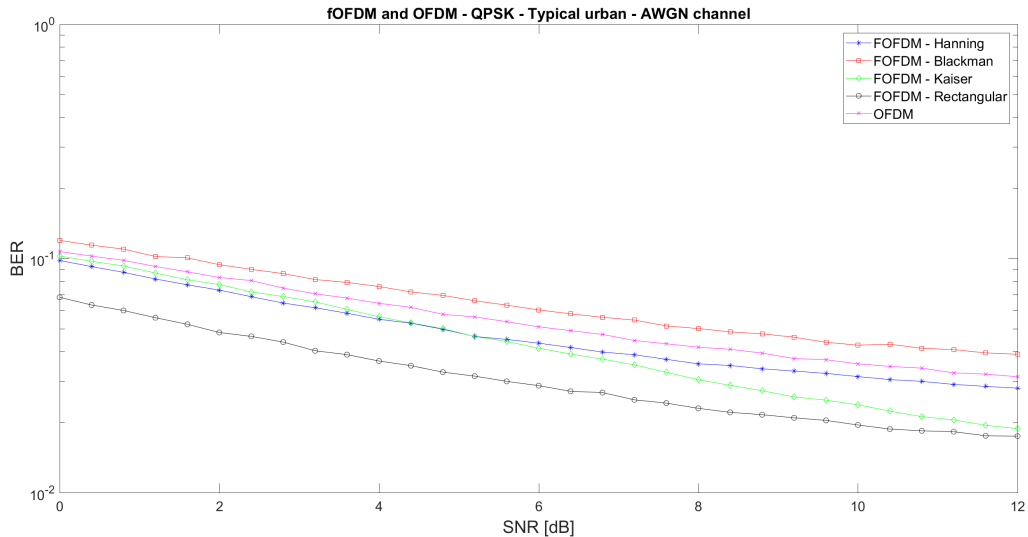


Figure 5.12: BER obtained by simulating the transmission of fOFDM, with different filters, and OFDM symbols.

the cyclic prefix.

The cyclic prefix consists of redundant information, which makes equalization much simpler and alleviates the multipath propagation effects.

fOFDM inherits this feature. However, the filtering, inherent to fOFDM, contributes for a higher ISI, which may significantly degrade communication performance under multipath propagation. Therefore, it is of interest to investigate how multipath propagation impacts fOFDM's BER.

HERMES already has some implemented channel models that follow COST-259 [23]. The typical urban and rural area scenarios were simulated and the results are presented in Figures 5.12 and 5.13.

In Figure 5.12, the results obtained in the typical urban channel model are portrayed. This model emulates the effects of towns where buildings have nearly uniform heights and densities [23].

The rectangular window had the best results while the Blackman window was the worst.

Next, Figure 5.13 exhibits the results obtained from a rural channel model. This model describes an environment with few buildings, such as farms and fields, which originates long delays, augmenting the BER degrading caused by multipath propagation.

In this scenario, the Blackman filter was the better option for fOFDM, while the other filters' performances were much worse.

As it can be seen in Figures 3.6 and 3.7, there is a trade-off between the window's impact on the filter time and frequency responses. Therefore, as shown by the simulations, the sharpest window (rectangular) or the window with the lowest OOB (Blackman) will have considerably different results depending on the channel.

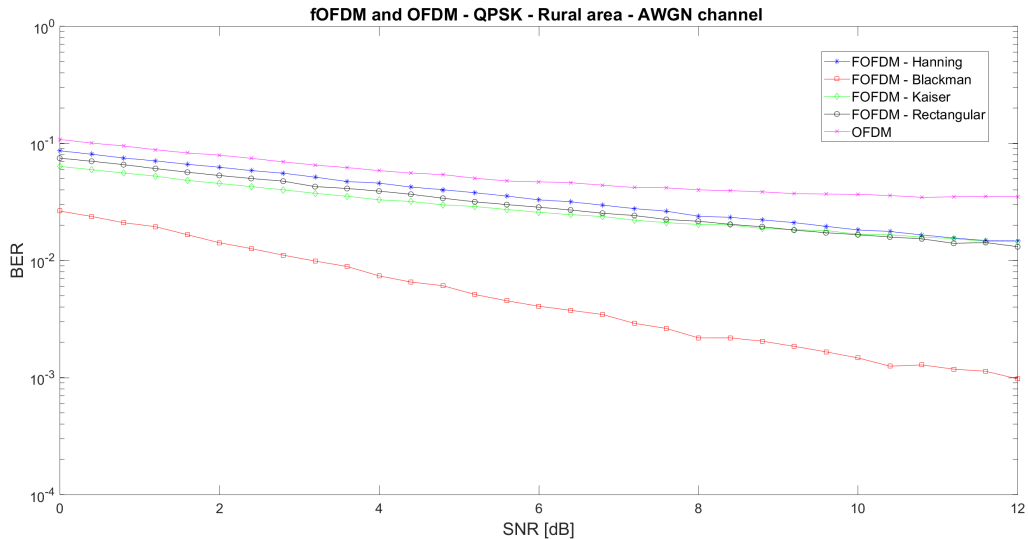


Figure 5.13: BER obtained by simulating the transmission of fOFDM, with different filters, and OFDM symbols.

Since the Blackman window has the best time decay, it will be less affected by the rural area’s long channel impulse response, when compared to the other windows. On the other hand, the rectangular window will have a better performance at the typical urban environment, which has a shorter impulse response, since the window’s sharp frequency response will be better equalized.

In the next sections, an intermediary window was picked for generating the FIR filters, which is the Hanning window.

5.3 Synchronous transmission under adjacent-channel interference

Throughout this section, the analyzed signals were generated according to the parameters in table 5.2.

The concept of filtering an OFDM signal comes into play with a goal, among others, of achieving a better BER when there’s interference.

In 5G, a large increase in the number of transmitting devices is expected. This is due to more human users acquiring mobile devices, but also the arrival of IoT. IoT will add many devices in the network, and there will be large amounts of machine-to-machine communication, increasing the data load on the network. When so many devices will be transmitting together, it is of interest to investigate solutions for mitigating the perform decreases that comes together with interference.

In this section, fOFDM performance under adjacent-channel interference is investigated and compared with OFDM. In this round of simulations, there are no other motives for performance degradation beyond interference and the conditions set in Table 5.2. Moreover, the transmission is synchronous between symbols.

Table 5.2: Parameters table.

Parameters	Value/Description
FFT size	512
Useful subcarriers	400
Subcarriers spacing	15kHz
Channel model	Unitary
User speed	36km/h
Modulation	QPSK
Cyclic Prefix length	$(1/8)512 = 64$
fOFDM Parameters	Value/Description
Filter window	Hanning
Filter order	20000

When the transmitted signal and the adjacent-channel interference have the same amount of transmit power, fOFDM and OFDM have similar performances, as shown by Figure 5.14. In addition, expanding the guard band between signals, by small amounts, will not considerably improve the transmission performance.

However, when the interfering signal has a power 10 dB higher than the desired signal, as seen in Figure 5.15, the schemes' behavior begin to differ.

Though fOFDM may filter out part of the ICI, the filtering process disrupts orthogonality in time, by making the signal longer than an unfiltered OFDM signal. This is a trade-off in this scheme. Therefore, when synchronous communication is available, unfiltered OFDM has time orthogonality and will perform better under interference.

5.4 Asynchronous transmission under adjacent-channel interference

Time synchronization is critical in OFDM's success. It makes OFDM symbols orthogonal among themselves in time and in frequency. Therefore, it is not possible to send OFDM symbols without global synchronization, in the same OFDM system.

fOFDM proposition is to enable asynchronous transmission between users that are allocated to different sub-bands. Therefore, it should be possible to have totally independent systems in each sub-band.

It is important to notice that there still must be synchronization between users sharing the same sub-band. Nonetheless, fOFDM will provide more flexibility than OFDM.

Throughout this section, the analyzed signals were generated according to the parameters in table 5.2.

By analyzing the results obtained in Figures 5.15 and 5.16, it is possible to verify how sensitive

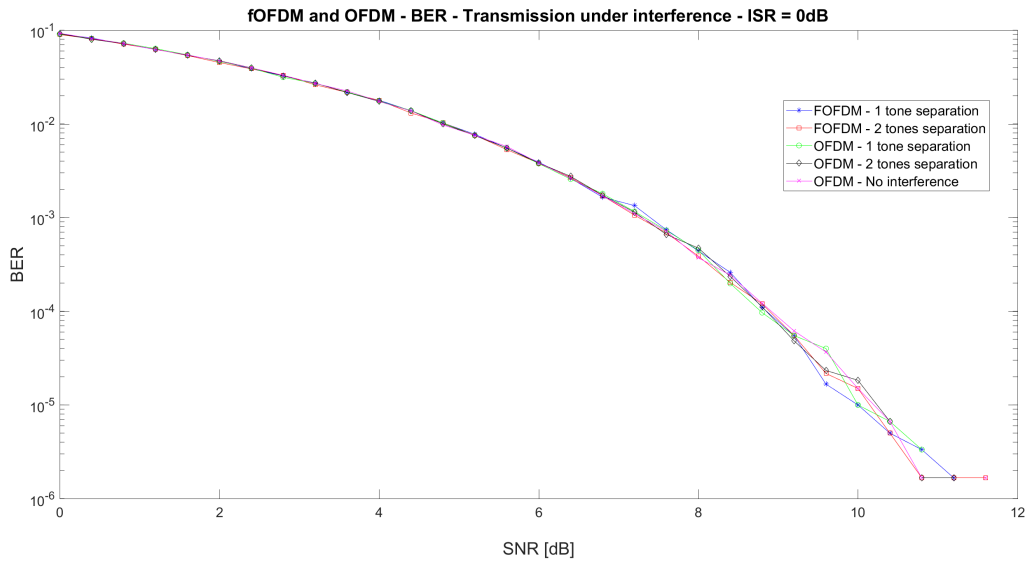


Figure 5.14: BER obtained by simulating OFDM and fOFDM symbols transmissions under interference with a single tone guard band between main signal and interfering signal. $ISR = 0\text{dB}$.

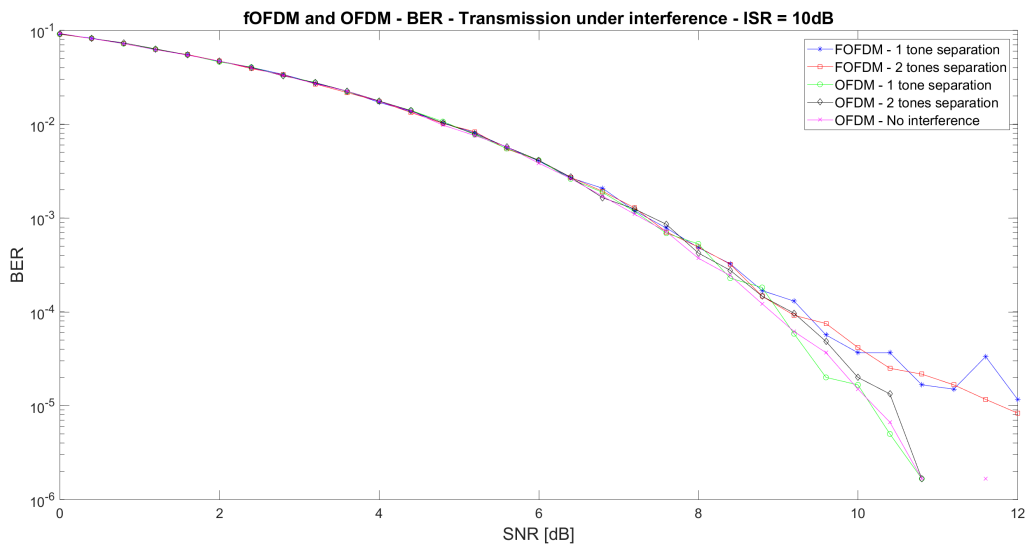


Figure 5.15: BER obtained by simulating OFDM and fOFDM symbols transmissions under interference with a single tone guard band between main signal and interfering signal. $ISR = 10\text{dB}$.

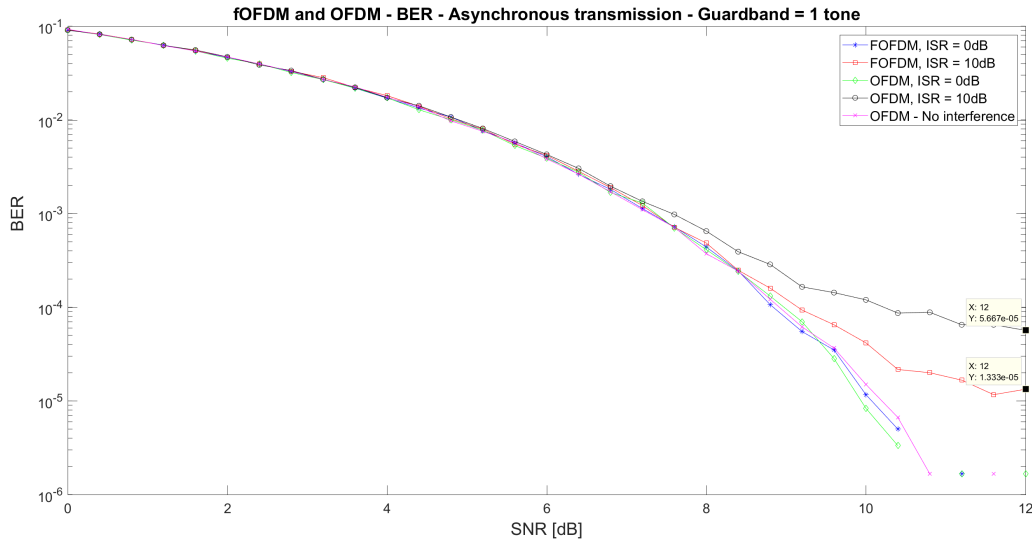


Figure 5.16: BER obtained by simulating OFDM and fOFDM symbols asynchronous transmissions under interference with a half-symbol delay present on the interfering signal. Guard band = 1 tone.

OFDM is to the loss of time synchronization.

When synchronous transmissions were simulated, Figure 5.15, OFDM's BER was kept almost unaltered, even when the ISR was increased by 10dB. In contrast, fOFDM's BER had a noticeable increase when the ISR was increased.

On the other hand, when time synchronization was broken, OFDM's performance was degraded while fOFDM's suffered considerably less, as depicted by Figure 5.16. This situation illustrates why fOFDM may be used for asynchronous transmission across sub-bands.

Moreover, fOFDM's has its performance enhanced proportionally to the increase of the guard band between signals. As can be seen in Figures 5.17 and 5.18, the guard band's expansion decreased the BER, approaching the best case scenario, which is OFDM without interference. In addition, OFDM is not expressively benefited by the guard band enlargement.

These results goes in accordance with the literature, [3, 9, 24]. However, [3, 9, 24] do not expose results about OFDM under asynchronous transmissions with interference. Only fOFDM is investigated under such circumstances and compared to OFDM in a scenario without interference.

Therefore, investigating how OFDM would perform in diverse scenarios was desired.

It may be concluded OFDM's performance is mostly influenced by synchronism in transmission. If global synchronization is not possible or if it is undesired, OFDM will behave poorly.

fOFDM's behavior is dependant on the ISR. However, this situation may be improved by enlarging the guard band between transmitted symbols by small amounts. If the ISR is high and it is not possible to allocate some tones as guard bands between sub-bands, fOFDM's BER will be high.

fOFDM's main advantages are its low OOB and the possibility of sending asynchronous

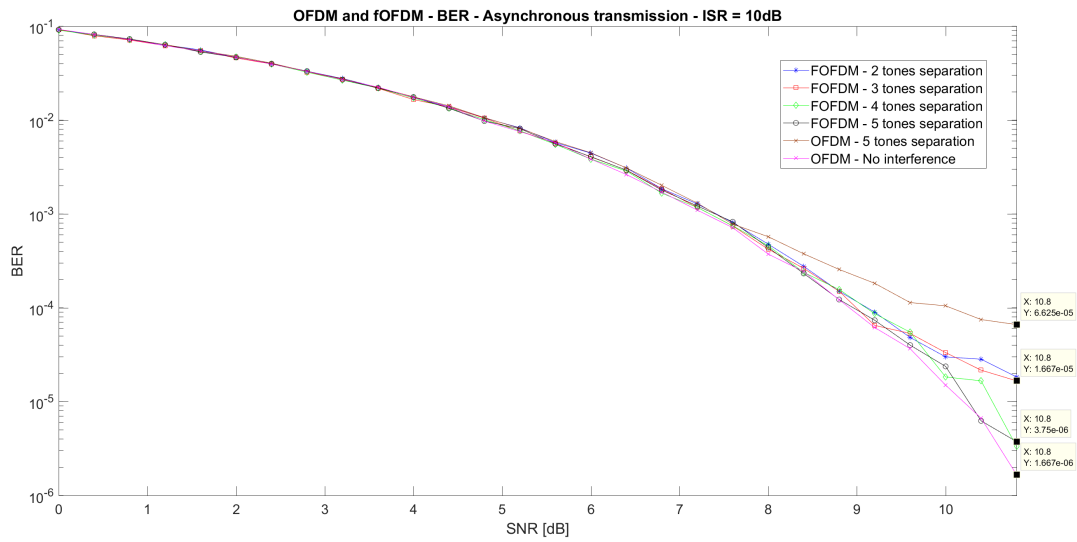


Figure 5.17: BER obtained by simulating OFDM and fOFDM symbols asynchronous transmissions under interference with a half-symbol delay present on the interfering signal. Multiple guard bands were simulated.

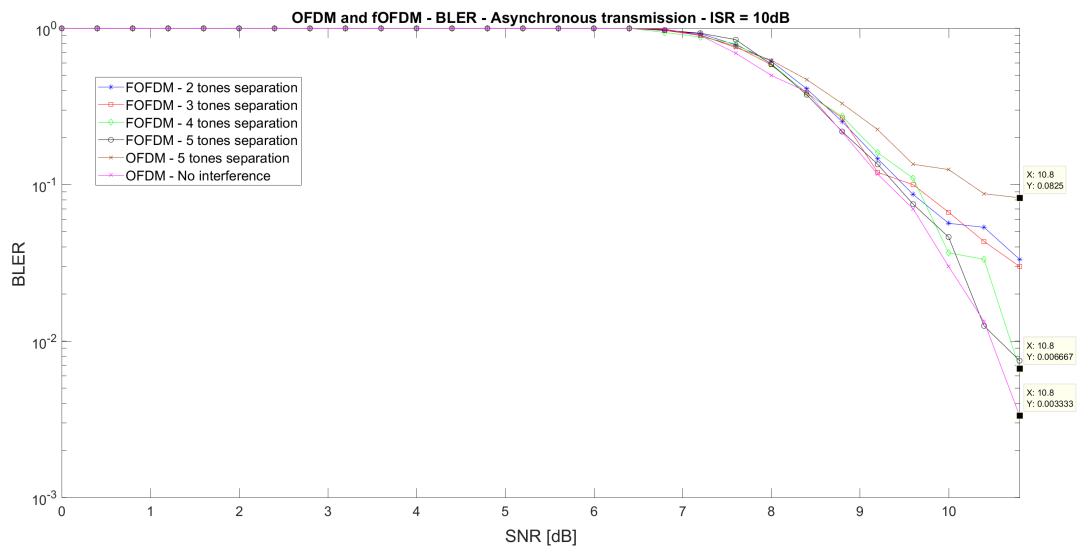


Figure 5.18: BLER obtained by simulating OFDM and fOFDM symbols asynchronous transmissions under interference with a half-symbol delay present on the interfering signal. Multiple guard bands were simulated.

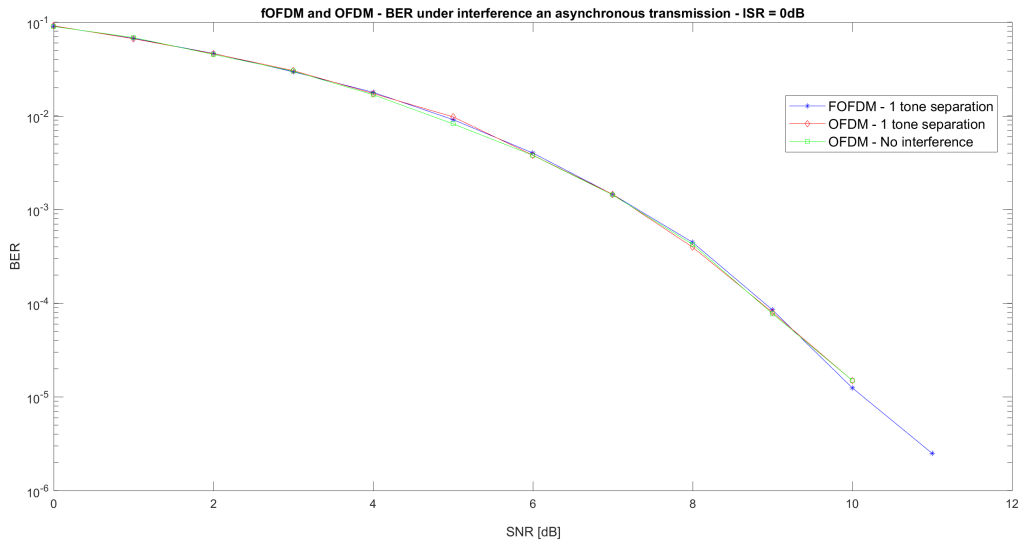


Figure 5.19: BER obtained by simulating OFDM and fOFDM symbols transmissions under interference with a single tone guard band between main signal and interfering signals. $ISR = 0\text{dB}$.

symbols across sub-bands.

With a low OOB, fOFDM allows the use of smaller guard bands, when compared to OFDM. Nowadays, LTE reserves 10% of the bandwidth as guard band. With fOFDM, it is possible to allocate small tones as guard band, which have the same length as the subcarrier spacing (15kHz in LTE). This feature increases the overall spectral efficiency, which is an express 5G goal.

The asynchronism is enabled as a filtering consequence. The filtering operation breaks the time orthogonality, once provided by OFDM. However, the filters are designed to compensate part of the performance loss due to orthogonality disruption while enabling asynchronous transmission across sub-bands.

It is also desirable to investigate the effects caused by raising the ISR, while the guard band is fixed, when interference and asynchronism are involved. Next, Figures 5.19, 5.20 and 5.21 display these results.

In Figure 5.19, fOFDM and OFDM present similar results. One possible conclusion is, when the SIR is only 0dB, OFDM's OOB is low enough so it affects only a few subcarriers. Hence, OFDM's performance will be as good as fOFDM's in no-interference scenarios, even with such a small guard band as 1 tone (15kHz).

Nonetheless, when the ISR is raised to 10dB, the schemes' performances begin to contrast. FOFDM, with a lower OOB, is more resilient to the interference than OFDM. The improvement upon the BER is now considerable, as portrayed by Figure 5.20.

The moment the ISR becomes even higher, 20dB, fOFDM's and OFDM's BER will both be heavily affected. Both schemes will have considerably high BERs, even though the fOFDM will have a superior performance 5.21. Even when increasing the guard band to 2 tones (30kHz), which still is a small guard band, the schemes will continue to have a bad performance when the ISR is

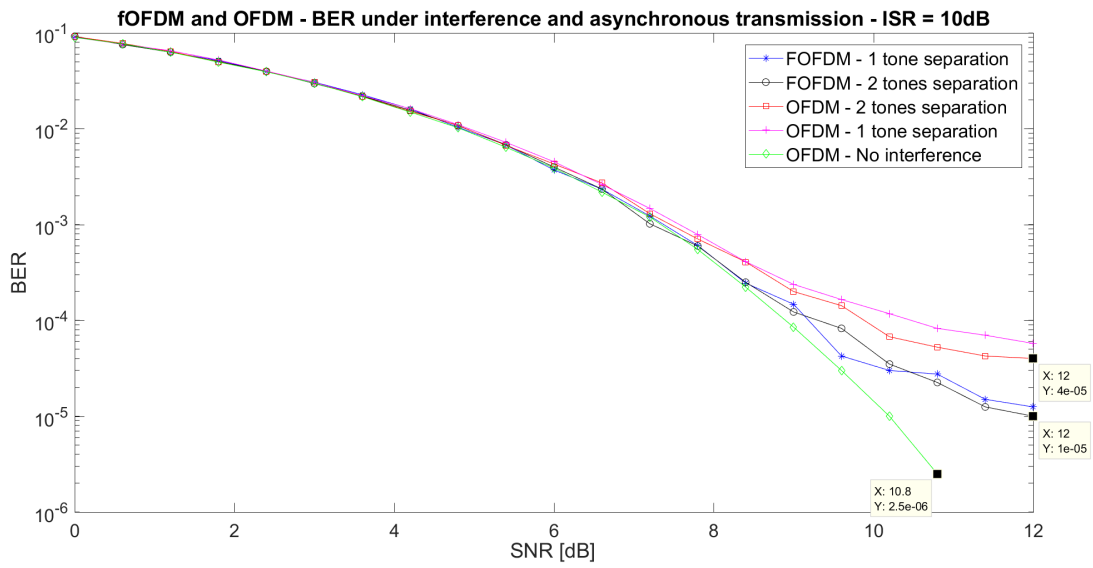


Figure 5.20: BER obtained by simulating OFDM and fOFDM symbols transmissions under interference with a two-tones guard band between main signal and interfering signals. $ISR = 10\text{dB}$.

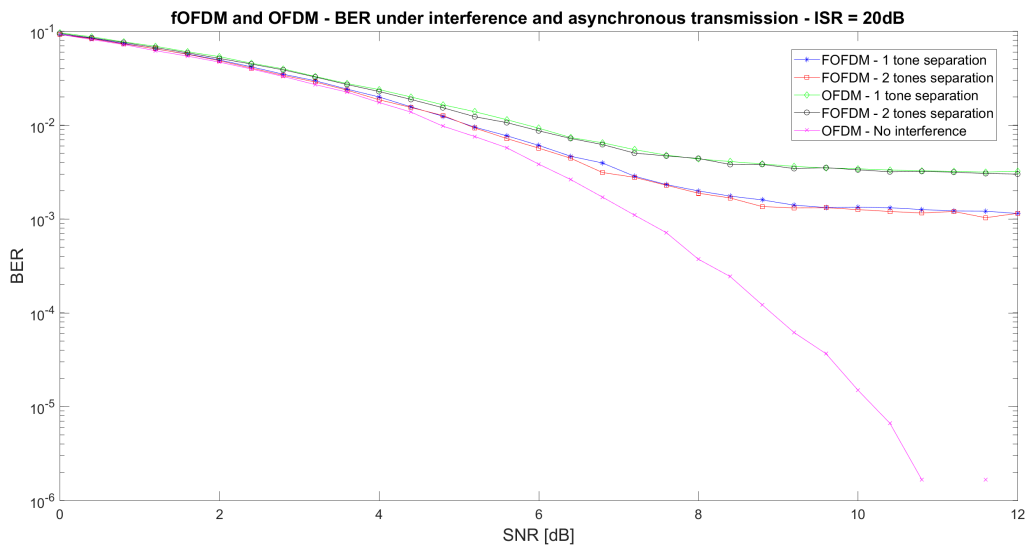


Figure 5.21: BER obtained by simulating OFDM and fOFDM symbols transmissions under interference with a two tones guard band between main signal and interfering signals. $ISR = 20\text{dB}$.

so high.

The interference causes the appearance of an error floor. For a given guard band, the error floor is an inferior limit for the BER. This explains why the schemes' BER and BLER curves stops decreasing along with the SNR after a certain SNR value.

Chapter 6

Conclusions

Filtered OFDM provides features that are not available on today's 4G-LTE. It is designed to support many heterogeneous applications along with a higher spectral efficiency.

This work studied fOFDM extensively by making use of the HERMES computational simulator.

When looking at fOFDM characteristics, explained at chapters 1 and 2, it is easy to see what fOFDM brings to the table. However, it was still of interest to evaluate its performance under diverse circumstances in order to see if it can replace its successful predecessor, OFDM.

Chapter 5 contains the results of various fOFDM studies. Analyzing the obtained results, it is possible to verify some of fOFDM features.

The simulations showed fOFDM, in fact, has a lower OOB than OFDM. This feature improves spectrum utilization, making it possible to reduce the amount of bandwidth allocated as guard bands.

In addition, it enables transmission without global synchronization, by dividing the frequency spectrum into sub-bands. The simulations show OFDM performs poorly under asynchronous transmission when the ISR is high, while fOFDM achieves performances similar to no-interference scenarios, simply by allocating small tones as guard bands.

These features go hand in hand with 5G's requirements, which are a flexible system, that supports a large number of heterogeneous applications, with different requirements such as ultra-low latency transmission and low power consumption.

Therefore, fOFDM is a promising candidate as part of the complete solution that will take mobile communication systems to the next generation.

6.1 Future works

In this work, the simulated under interference transmissions contained two sub-bands. In each sub-band, there was an fOFDM or an OFDM system in it, with the same numerology. Hence, it is of interest to simulate scenarios with a larger number of sub-bands, with different numerology,

e.g. different CP lengths, modulations, symbol sizes, subcarrier spacing. It is also of interest to allocate some of the sub-bands to systems with other schemes than OFDM, such as single carrier schemes, that may have practical application.

Even though fOFDM seems like a natural transition from OFDM, fOFDM requires more computational power than unfiltered OFDM, due to its flexibility. When fOFDM is concerned, it is of interest to calculate the resources allocation for each sub-band in an optimized way. Following, there are the filtering operations.

Even though fOFDM seems like a natural transition from OFDM, fOFDM's online filter generation may be complex. The filters are designed according to the channel and the required numerology. Hence, fOFDM will require more computational power than standard OFDM. Quantifying how much more computational power fOFDM will require, in comparison to OFDM, and developing solutions for optimizing these calculations is desirable.

In addition, uplink and downlink designs are also essential. Nowadays, in LTE, uplink and downlink are different, due to the complexity of providing multi-user access. It is of interest to study how complex uplink and downlink will be in fOFDM and if it is possible to implement both similarly.

Channel coding is another aspect that requires attention. In this work, fOFDM was studied in situations with no channel coding. It is necessary to investigate how channel coding affects fOFDM's performance.

It is also of interest to study how fOFDM is affected by the radio frequency (RF) impairments, caused by the analog hardware imperfections. This subject is investigated by [18].

By the time this work has been written, 5G has not been officially standardized. However, if fOFDM is designated as the standard scheme, there will be space for many studies and works on this field.

BIBLIOGRAPHY

- [1] ITU-R, “IMT Vision – Framework and overall objectives of the future development of IMT for 2020 and beyond,” tech. rep., ITU-R, Setembro 2015. Accessed in January 2018.
- [2] J. Armstrong, “5G - OFDM for Optical Communications,” *Journal of Lightwave Technology*, vol. 27, no. 31, 2009.
- [3] X. Zhang, M. Jia, L. Chen, J. Ma, and J. Qiu, “Filtered-OFDM-enabler for flexible waveform in the 5th generation cellular networks,” in *Global Communications Conference (GLOBECOM), 2015 IEEE*, pp. 1–6, IEEE, 2015.
- [4] I. ITU, “2134, requirements related to technical performance for imt-advanced radio interface (s),” *International Telecommunications Union*, 2008.
- [5] V. Chakravarthy, A. S. Nunez, J. P. Stephens, A. K. Shaw, and M. A. Temple, “TDCS, OFDM, and MC-CDMA: a brief tutorial,” *IEEE Communications Magazine*, vol. 43, no. 9, pp. S11–S16, 2005.
- [6] A. N. Barreto, B. Faria, E. Almeida, I. Rodriguez, M. Lauridsen, R. Amorim, and R. Vieira, “5G–Wireless Communications for 2020,” *Journal of Communication and Information Systems*, vol. 31, no. 1, 2016.
- [7] Rohde Schwarz, “5G Waveform Candidates.” https://cdn.rohde-schwarz.com/pws/dl_downloads/dl_application/application_notes/1ma271/1MA271_0e_5G_waveform_candidates.pdf, October 2016. Accessed in January, 2018.
- [8] “Rel-15 success spans 3GPP groups.” http://www.3gpp.org/news-events/3gpp-news/1965-rel-15_news. 3rd Generation Partnership Project, Accessed in June, 2018.
- [9] X. Zhang, L. Chen, J. Qiu, and J. Abdoli, “On the waveform for 5g,” *IEEE Communications Magazine*, vol. 54, no. 11, pp. 74–80, 2016.
- [10] D. A. Wiegandt, C. Nassar, and Z. Wu, “The elimination of peak-to-average power ratio concerns in ofdm via carrier interferometry spreading codes: A multiple constellation analysis,” in *System Theory, 2004. Proceedings of the Thirty-Sixth Southeastern Symposium on*, pp. 323–327, IEEE, 2004.
- [11] R. W. Chang, “Orthogonal frequency multiplex data transmission system,” Jan. 6 1970. US Patent 3,488,445.

- [12] J. Salz and S. Weinstein, “Fourier transform communication system,” in *Proceedings of the first ACM symposium on Problems in the optimization of data communications systems*, pp. 99–128, ACM, 1969.
- [13] A. Peled and A. Ruiz, “Frequency domain data transmission using reduced computational complexity algorithms,” in *Acoustics, Speech, and Signal Processing, IEEE International Conference on ICASSP’80.*, vol. 5, pp. 964–967, IEEE, 1980.
- [14] P. Weitkemper, J. Bazzi, K. Kusume, A. Benjebbour, and Y. Kishiyama, “On regular resource grid for filtered ofdm,” *IEEE Communications Letters*, vol. 20, no. 12, pp. 2486–2489, 2016.
- [15] P. Weitkemper, J. Bazzi, K. Kusume, A. Benjebbour, and Y. Kishiyama, “Adaptive filtered ofdm with regular resource grid,” in *Communications Workshops (ICC), 2016 IEEE International Conference on*, pp. 462–467, IEEE, 2016.
- [16] J. G. Proakis and D. G. Manolakis, *Digital Signal Processing Fourth Edition*. Academic Press, London, UK, 2007.
- [17] “HERMES.” <https://github.com/MWSL-UnB/HERMES>. Accessed in February, 2018.
- [18] Ornelas, G. C., “Simulação de formas de onda candidatas ao 5G na presença de imperfeições de RF e de múltiplas antenas.” Trabalho de conclusão de curso, Universidade de Brasília, 2017.
- [19] Rodrigues, A. A., “Análise comparativa de desempenho de formas de onda candidatas ao 5G.” Trabalho de conclusão de curso, Universidade de Brasília, 2016.
- [20] “Representação em banda-base de sinais passa-banda .” https://paginas.fe.up.pt/~sam/Tele2/apontamentos/Envolv_complexa.pdf. Universidade do Porto, Accessed in February, 2018.
- [21] Z. E. Ankarali, B. Peköz, and H. Arslan, “Flexible radio access beyond 5g: A future projection on waveform, numerology, and frame design principles,” *IEEE Access*, vol. 5, pp. 18295–18309, 2017.
- [22] X. Cheng, Y. He, B. Ge, and C. He, “A filtered ofdm using fir filter based on window function method,” in *Vehicular Technology Conference (VTC Spring), 2016 IEEE 83rd*, pp. 1–5, IEEE, 2016.
- [23] H. Asplund, A. A. Glazunov, A. F. Molisch, K. I. Pedersen, and M. Steinbauer, “The cost 259 directional channel model-part ii: macrocells,” *IEEE Transactions on Wireless Communications*, vol. 5, no. 12, 2006.
- [24] J. Abdoli, M. Jia, and J. Ma, “Filtered ofdm: A new waveform for future wireless systems,” in *Signal Processing Advances in Wireless Communications (SPAWC), 2015 IEEE 16th International Workshop on*, pp. 66–70, IEEE, 2015.